

AD-A176 445

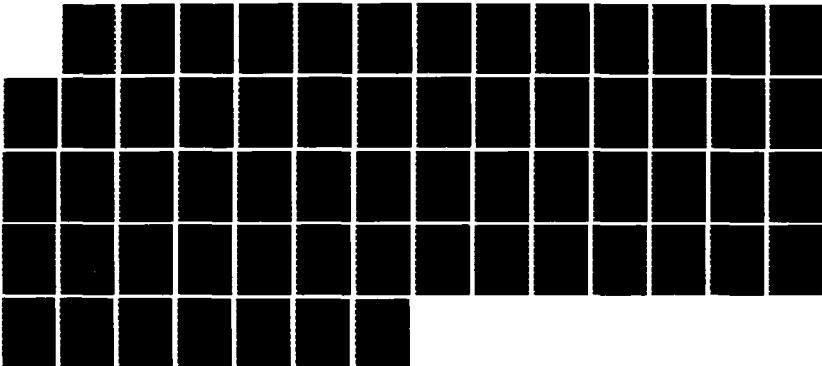
SYNCHROTRON RADIATION STUDIES OF MBE-GROWN
SEMICONDUCTOR AND METAL SURFAC. (U) IBM THOMAS J WATSON
RESEARCH CENTER YORKTOWN HEIGHTS NY R LUDEKE 08 DEC 86
ARO-19030 12-EL DAAG29-83-C-0026

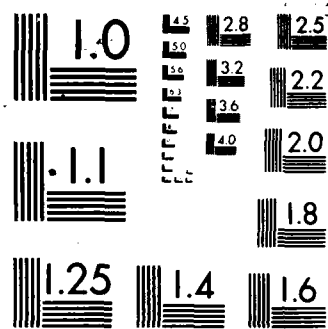
1/1

UNCLASSIFIED

F/G 20/12

NL





MICROCOPY RESOLUTION TEST CHART
NATIONAL BUREAU OF STANDARDS-1963-A

2

UNCLASSIFIED

SECURITY CLASSIFICATION OF THIS PAGE (When Data Entered)

AD-A176 445

REPORT DOCUMENTATION PAGE		READ INSTRUCTIONS BEFORE COMPLETING FORM
1. REPORT NUMBER ARO 19030.12-EL	2. GOVT ACCESSION NO. N/A	3. RECIPIENT'S CATALOG NUMBER N/A
4. TITLE (and Subtitle) Synchrotron Radiation Studies of MBE-Grown Semiconductor and Metal Surfaces and Interfaces	5. TYPE OF REPORT & PERIOD COVERED Final	
	6. PERFORMING ORG. REPORT NUMBER	
7. AUTHOR(s) R. Ludeke	8. CONTRACT OR GRANT NUMBER(s) DAAG 29-83-C-0026	
9. PERFORMING ORGANIZATION NAME AND ADDRESS		10. PROGRAM ELEMENT, PROJECT, TASK AREA & WORK UNIT NUMBERS
11. CONTROLLING OFFICE NAME AND ADDRESS U. S. Army Research Office Post Office Box 12211 Research Triangle Park, NC 27709		12. REPORT DATE Dec. 8, 1986
14. MONITORING AGENCY NAME & ADDRESS (if different from Controlling Office)		13. NUMBER OF PAGES
		15. SECURITY CLASS. (of this report) Unclassified
		15a. DECLASSIFICATION/DOWNGRADING SCHEDULE
16. DISTRIBUTION STATEMENT (of this Report) Approved for public release; distribution unlimited.		
17. DISTRIBUTION STATEMENT (of the abstract entered in Block 20, if different from Report) NA		
18. SUPPLEMENTARY NOTES The view, opinions, and/or findings contained in this report are those of the author(s) and should not be construed as an official Department of the Army position, policy, or decision, unless so designated by other documentation.		
19. KEY WORDS (Continue on reverse side if necessary and identify by block number) 1. GaAs, 2) InP, 3) oxidation, 4) transition metals; 5) substitutional impurities, 6) Schottky barrier; 7) Sb; 8) ordered overlayer; 9) core level spectroscopy, 10) photoemission, 11) inverse photoemission, 12) line shape analysis (spectral decompositions).		
20. ABSTRACT (Continue on reverse side if necessary and identify by block number) The work for the contract period addressed the physics and chemistry underlying the formation of the electronic structure at semiconductor-oxide and semiconductor-metal interfaces. Using photoemission spectroscopy excited with synchrotron radiation, and inverse photoemission spectroscopy a new oxidation model has been proposed for GaAs and InP. Extensive studies of transition metals deposited on GaAs and InP led to the first concrete identification of interface states responsible for the formation of the Schottky barrier, namely d-derived impurity levels of transition metal atoms in the semiconductor.		

DIR
ELECTE
FEB 6 1987
A

OTIC FILE COPY

RESEARCH SUMMARY

The main thrust of research under this contract was directed towards the understanding of the electronic structure at the developing interface between a semiconductor and its oxide or a metal. The electronic structure at the interface, which determines for instance band offsets and the position of the Fermi level through defect structures, is generally finalized after a few monolayers of the second medium have been deposited on the semiconductor. This observation, which was substantiated by work under this contract at least for the metal-semiconductor interface, allows the study of the development and ultimate stabilization of the electronic properties by surface-sensitive electron spectroscopies such photoemission and inverse photoemission. Both spectroscopies rely on the selectively variable escape depth of electrons in the 0.3 to 2 nanometer range. Synchrotron-excited photoemission, performed at the National Synchrotron Light Source, Brookhaven, N.Y., proved particularly advantageous in these studies because of the wide range of adjustable photon energies and high resolution of the IBM installed instrumentation allowed core level studies over a broad range of binding energies. The high resolution of better than 200 meV, achieved with a novel 6/10 meter toroidal grating monochromator together with a unique display electron spectrometer and the development of computer-aided curve fitting routines permitted unprecedented determinations of core level components that are necessary to study and understand the interfacial chemistry which ultimately determines the electronic structure of the interface.

The principal scientific achievements lie in the elucidation of the oxidation process of GaAs and InP and the formation and spectroscopic identification of metal-induced interface states that determine the Schottky barrier for transition metals deposited on GaAs and InP. A short discussion with reference to published results will be given next. We have also recently started to investigate the electronic structure of ordered overlayers of Sb on GaAs and InP. Preliminary results will be briefly discussed as well.

a) Oxidation of GaAs and InP.

Many previous studies of the oxidation of cleaved (110) surfaces of GaAs generally concluded that the oxidation proceeds in a chemically homogeneous fashion (i.e. stoichiometrically) which is limited in the absence of ionizing radiation to a surface oxide. Our results (ref. 1,3,5 and 11) clearly showed that the oxidation of GaAs is both spatially and chemically inhomogeneous, that is, the oxidation from the earliest stages on proceeds with breakage of back bonds and separate oxides of Ga and As form. Similar "bulk" oxidation was observed for InP. However, the resulting oxide is chemically more homogeneous in that a predominantly single phase native oxide forms of approximate chemical formula InPO_4 (ref. 11). Annealing this oxide enhanced its stoichiometry. These studies included the first observation of structure (chemical shifts) in the O-1s core level

spectrum of an oxide (ref. 5) and the first use of variable electron escape depth to study sub-surface chemical processes (ref. 3).

b) Transition metals on GaAs and InP.

The underlying mechanism for the formation of the Schottky barrier is the presence of interface states that pin the Fermi level in the band gap region of the semiconductor. Although spectroscopically observable in special cases, their origin has never before been unequivocally identified, although a variety of native defects, such as vacancies and antisites, and precipitates of the group V elements, have been implicated. Taking advantage of the large photoionization cross sections of the d-electron valence levels of the transition metals, we have been able to detect band gap emission emanating from d-orbitals of the transition metal atom for coverages above 1/100 of a monolayer. Complimentary results, using inverse photoemission spectroscopy, were obtained for the empty band gap states generated by the transition metal atoms. The Fermi level, as expected, would lie in between the filled and empty bands of interface states (ref. 9, 10, 12). At a coverage near 1/10 of a monolayer all band bending had effectively stopped and the Schottky barrier height did not appreciably change with further coverage (refs. 8, 12). The results indicated that the Schottky barrier determining interface states were formed long before a metallic character of the transition metal overlayer formed. Detailed core level studies indicated that considerable chemistry was occurring during all stages of growth, with the predominant reaction appearing to be a replacement of the surface Ga sites with a transition metal. The defect or impurity level thus generated has a well known bulk-equivalent, the transition metal substitutional impurity, with known "deep" impurity levels in the band gap region of most semiconductors. A good correlation of the photoemission spectrum and the corresponding acceptor and donor levels of the substitutional impurity was observed. The actual Schottky barrier determining level is believed to be a more complicated impurity, but which has spectroscopic similarities to the simple impurity. Appendix A, a copy of reference 12, gives more details on the experimental evidence and details of the model. The model is not universal; yttrium for example does not form isolated impurity levels in the bulk band gap, yet it produces a Schottky barrier. This barrier is formed considerably slower than for the other transition metals, indicating that interface states of another origin determine the properties of the Y/GaAs Schottky barrier. Details of this unusual system can be found in Appendix B, which is a preprint of an article recently submitted to the Physical Review.

c) Ordered Sb layer on GaAs and InP.

Prior work on room temperature deposited Sb monolayers on the cleaved GaAs(110) surface was interpreted in terms of a perfect, ordered overlayer which left the GaAs "unpinned", and perhaps somewhat inert to further contaminations. Such a passivation would be of considerable importance to the control of interfacial electronic properties. Our recent studies revealed, however, that the

Sb/GaAs interface is not passivated, but can be made "unpinned" only if the Sb monolayer, or fraction thereof, is deposited or annealed at temperatures near 300 C. Treated at that temperature, the Sb monolayer is perfect, but exhibits a surface state band 280 meV above the GaAs valence band maximum which pins the Fermi level at that position for p-type GaAs. Deposition at room temperature for coverages beginning at below a monolayer always produce band bending (a Schottky barrier) on both n- and p-type GaAs. Annealing the overlayer reduces the band bending to the above mentioned value on p-type GaAs. Any subsequent Sb deposition and or that of a metal re-establishes a Schottky barrier. Core level spectra indicate that the band bending is due to Sb atoms bonding on top of the ordered layer. Annealing such a sample results in the removal of the additional Sb atoms either through re-evaporation or surface diffusion to an uncovered GaAs lattice site, which re-establishes the near flat-band condition. The experiments further demonstrate that the heat of deposition (which is sufficient to break up the condensed Sb_4 molecules) is insufficient to generated intrinsic defects in the GaAs. Such a mechanism is frequently invoked to explain the formation of interface states which determine Schottky barriers. Appendix C shows a detailed description of this work.

PUBLISHED RESEARCH

1. Oxidation of GaAs (110): New Results and Models, G. Landgren, R. Ludeke, J. F. Morar, Y. Jugnet and F. J. Himpsel, Phys. Rev. Rapid Commun., **B30**, 4839 (1984).
2. Morphological and Chemical Considerations for the Epitaxy of Metals on Semiconductors, R. Ludeke, J. Vac. Sci. Technol., **B2**, 400 (1984).
3. The Oxidation of GaAs(110): A Reevaluation, G. Landgren, R. Ludeke, Y. Uugnet, J. F. Morar, and F. J. Himpsel, J. Vac. Sci. Technol. B **2**, 351 (1984).
4. A Critical Comparison Of The Techniques Used To Characterize The Crystallography Of An Interface: Pd on MBE grown GaAs (100), J.-P. Delrue, M. Wittmer, T. S. Kuan and R. Ludeke, Mat Res. Soc. Symp. Proc., vol. 37, 455 (1985).
5. O-1s Core Level Studies of the Oxidation of GaAs (110), G. Hughes, R. Ludeke, J. F. Morar and J. L. Jordan, J. Vac. Sci. Technol., **B3**, 1079 (1985).
6. MBE Surface and Interface Studies, R. Ludeke, R. M. King and E.H.C. Parker, Chapter 16 Interface Formation, in The Technology and Physics of Molecular Beam Epitaxy, edited by E. H. C. Parker, (Plenum Publishing Corp., NY, 1985), pp.555-628.
7. The Effects of Microstructure on Interface Characterization, R. Ludeke, Surf. Science **168**, 290 (1986).
8. Electronic Properties and Chemistry of Ti/GaAs and Pd/GaAs Interfaces, R. Ludeke and G. Landgren, Phys. Rev. **B33**, 5526 (1986).
9. Metal-Derived Bandgap States: Ti on GaAs (110), R. Ludeke, D. Straub, F. J. Himpsel and G. Landgren, J. Vac. Sci. Technol. **A4**, 874 (1986).
10. Transition Metals on GaAs: A Case for Extrinsic Surface States, G. Hughes, R. Ludeke, F. Schäffler and D. Rieger, J. Vac. Sci. Technol. **B4**, 924 (1986).
11. O-1s Studies of the Oxidation of InP(110) and GaAs(110) Surfaces, G. Hughes and R. Ludeke, J. Vac. Sci. Technol. **B4**, 1109 (1986).
12. An impurity model for the Schottky Barrier: transition metals on III-V Compound Semiconductors, R. Ludeke, G. Hughes, F. Schäffler, F.J. Himpsel, D. Rieger, D. Straub and G. Landgren, Proc. Int'l. Conf. on Physics of Semiconductors, Stockholm 1986, in press.

13. Metal-induced impurity states at the InP/transition metal interface, F. Schäffler, W. Drube, G. Hughes, R. Ludeke, D. Rieger and F.J. Himpsel, submitted to J. Vac. Sci. Technol.
14. A comparative study of Y and other Transition Metals on GaAs, F. Schäffler W. Drube, G. Hughes, R. Ludeke and F.J. Himpsel, submitted to Phy. Rev. B.
15. The Sb/GaAs Interface: A Re-evaluation, F. Schäffler, R. Ludeke, A. Taleb-Ibrahimi and G. Hughes, submitted to Phys. Rev. Rapid Commun.
16. Metal-semiconductor Interfaces: the Role of Structure and Chemistry, R. Ludeke, NATO Workshop, in preparation.

AN IMPURITY MODEL FOR THE SCHOTTKY BARRIER:
TRANSITION METALS ON III-V COMPOUND SEMICONDUCTORS.R. Ludeke, G. Hughes*, W. Drube, F. Schäffler, F.J. Himpsel,
D. Rieger, D. Straub+ and G. Landgren†.IBM T.J. Watson Research Center, P.O. Box 218, Yorktown Heights, N.Y.
10598, U.S.A.

ABSTRACT

We report the observation of filled and empty interface states derived from the interaction of transition metals (TMs) with GaAs. For Ti, V and Pd these states, attributed to impurity levels, determine the position of the interface Fermi level.

1. INTRODUCTION

The origin of the interface state responsible for the stabilization of the Fermi level at the metal-semiconductor interface has long been a controversial issue. Although a variety of sources have been proposed,¹⁻³⁾ spectroscopic evidence in support of any model has been lacking up to now. Evidence for interface states has been obtained previously by spectroscopic⁴⁾ and electrical⁵⁾ measurements, however no correlations with a specific mechanism, structural defect or chemical species could be made. In this work we report the observation of filled and empty interface states derived from the interaction of transition metals (TMs) with the GaAs surface, and suggest a possible origin - a substitutional TM impurity at the interface - based on spectroscopic evidence and changes in the interface chemistry.

2. EXPERIMENTAL DETAILS

The TMs were sublimed from wires or foils onto freshly cleaved GaAs(110) surfaces in vacuums of 10^{-10} Torr. Both n and p-type substrates, doped respectively with Si and Zn to $\sim 10^{18}$ cm⁻³ were used. The thickness was monitored with a quartz microbalance. Details of the experimental procedures, including the line shape analysis of the core level spectra are given elsewhere.⁶⁾ Inverse photoemission was used to probe the conduction band states and empty interface states. The technique consists of directing a monochromatic electron beam onto a surface and spectrally analyzing the resulting photon flux.⁷⁾

3. EXPERIMENTAL RESULTS

It has now been established that the TMs react strongly with GaAs and other semiconductor substrates.^{7,8)} This behavior is readily observed in the core level

photoemission spectra of the semiconductor. Fig. 1 depicts the evolution of the Ga and As 3d core level spectra as a function of Mn coverage. The experimental spectra (dots) have been decomposed into chemically shifted individual components by computer fitting routines.^{7,91} The spectra of the clean surface are made up of a bulk peak (large component) and a surface peak. The latter decreases with coverage of the TM. For coverages as low as 0.02 Å an additional chemically shifted peak can be observed in the Ga 3d core level spectrum; this structure is obvious in Fig. 1 for a coverage of 0.4 Å. This peak is attributed to elemental Ga, which diffuses to the surface of the growing Mn film. This behavior is strong evidence that an exchange reaction has occurred on the surface, with the TM (here Mn) replacing the Ga. The situation is less clear for the As since the emergence of a chemically shifted As component, obvious for a coverage of 3 Å, is disguised at the lower coverages by the surface peak. The general lack of experimental evidence for elemental As (except for Pd⁷) suggests that Ga is the predominantly replaced surface component, and that the As, both at the interface and as a diffused species, is predominantly bonded to the TM.

The spectral decomposition is necessary as well to accurately follow the shifts in kinetic energy with coverage of the bulk component, so that the resulting band bending and final positions of the Fermi level E_F can be ascertained.⁹¹ The positions in the band gap of E_F as a function of coverage for several TMs on GaAs(110) are shown in Fig. 2. We also indicate the final position of E_F for several other metals on the right hand ordinate. Three important conclusions can be drawn from the data: a) the final value of E_F (and the Schottky barrier) may vary by as much as 0.3 eV for different metals; b) the same final position of E_F is obtained independent of the doping type; and c) the band bending is essentially complete, except for Ag,⁹¹ near a coverage of 0.1 Å, which is below the coverage necessary to establish a metallic behavior of the overlayer. These observations are generally inconsistent with present Schottky barrier models, and we must look for a different origin of the interface states which determine E_F at the interface. The strong reactions with the TMs suggest states induced by a new chemical environment, i.e. of extrinsic origin, which are readily observed in the valence band spectra.

Fig. 3 depicts valence band spectra for clean GaAs and for the indicated coverages of V, Mn and Y. Strong spectral features are readily observed which originate from the d-electrons of the TMs. Difference spectra, obtained by subtracting the clean spectrum, are shown on the right of Fig. 3. The sharp spectral features are already discernible at coverages of ~ 0.01 Å (not shown) and suggest a unique chemical environment of the TM, at least at low coverages. Based on the core level spectra, the Ga substitutional site is a likely site for the TM, but requires additional confirmation. We can, however, draw the conclusion that the TMs induce filled interface states which overlap the valence band of GaAs, and in the case of Ti, V, Pd and to a lesser extent Mn, extend into the band gap, where the emission edge coincides with the position of E_F . This is more clearly shown in Fig. 4, which is a composite of difference spectra (solid lines) of the valence bands (VB), obtained by phototemission, and the conduction bands (CB), obtained by inverse

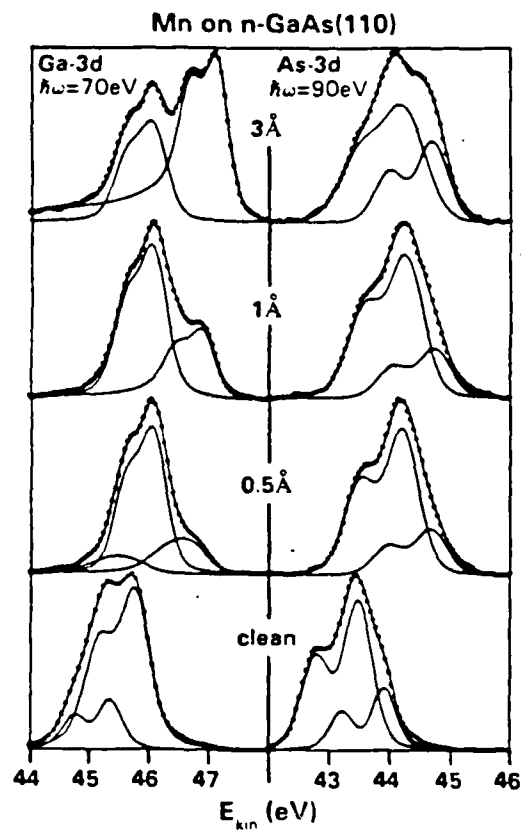


Figure 1

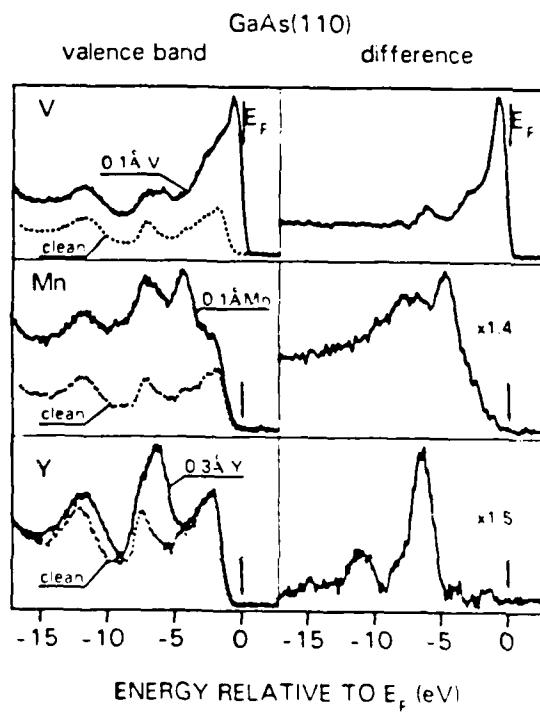


Figure 3

FERMI LEVEL AT GaAs(110) INTERFACE

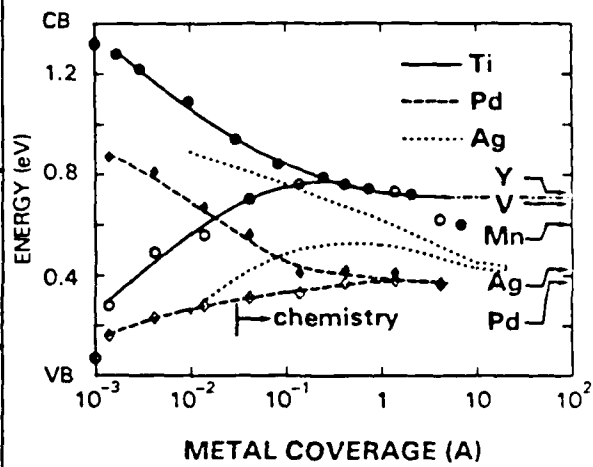


Figure 2

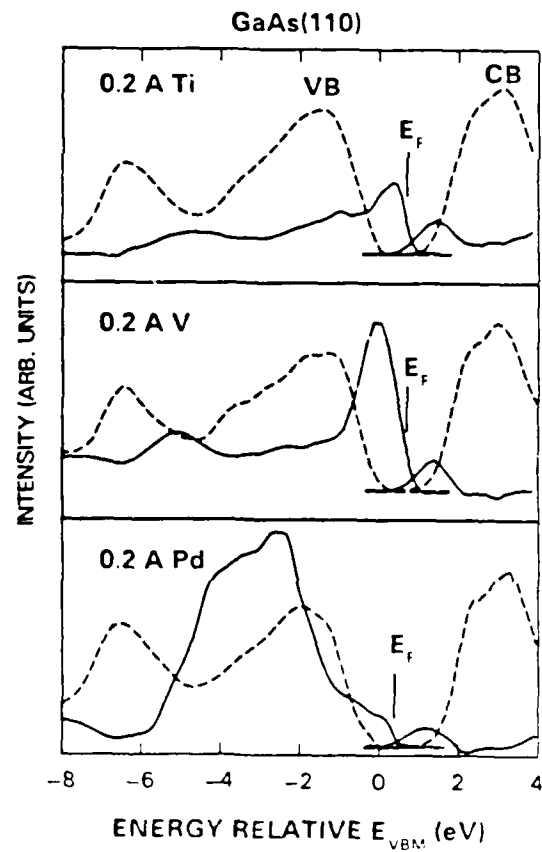


Figure 4

photoemission spectroscopy (IPS), following 0.2 Å of Ti, V and Pd. The dashed curves show the experimental spectra for the clean surface. The IPS results clearly show the existence of empty interface states derived from empty d-states, which extend into the band gap, and with the filled states determine the position of the E_F at the interface.

4. DISCUSSION AND CONCLUSIONS

The energetic positions of the emission peaks of the filled and empty interface states in the GaAs band gap for Ti and V (Fig. 4) coincide remarkably well with the ionized donor and acceptor levels of the respective TM substitutional impurity for GaAs,¹⁰ and thereby lend additional support for this type of defect. Donor states have not been observed for Mn in the band gap, which is consistent with our observations, and the bulk impurity levels for Pd have not yet been reported. Nevertheless, Mn and Y form pinning states which are not readily identifiable from our spectroscopic results. Y in a substitutional Ga site is not expected to produce donor states in the band gap, since its three valence electrons ($4d^1 5s^2$) will be in bonding orbitals, a notion consistent with the spectroscopic data. We speculate at this point that other reaction products, Ga for example, are the most likely source for the interface states responsible for the pinning of TMs which do not form d-derived interface states in the band gap. In addition, for all present cases, aggregates of TMs or other complexes with other type of defects cannot be ignored, especially at the larger coverages, for which the interface chemistry is complex.

Present addresses: *School for Physical Sciences, NIHE, Dublin, Ireland; *Mannesmann-Kienzle, D-7730 Villingen, Germany; †Institute for Microwave Technology, S-100 44 Stockholm, Sweden. This research was partially supported by the U.S. Army Research Office, under contract #DAAG29-83-C-0026 and carried out in part at the NSLS, Brookhaven National Laboratory.

REFERENCES

1. Spicer, W.E, Kendelewicz, T., Newman, N., Chin, K.K., Lindau, I., Surf. Sci. 168, 240 (1986)
2. Freeouf, J.L., and Woodall, J.M., Appl. Phys. Lett. 39, 727 (1981).
3. Heine, V., Phys. Rev. A138, 1689 (1965); Tersoff, J., Phys. Rev. Lett. 57, 465 (1984).
4. Bolmont, D., Chen, P., Sebenne, C.A., and Proix, F., Surf. Sci. 137, 280 (1984).
5. Chekir, F. and Barret, C., Appl. Phys. Lett. 45, 1212 (1984).
6. Ludeke, R. and Landgren, G., Phys. Rev. B33 5526 (1986); Ludeke, R., Straub, D., Himpsel, F.J., and Landgren, G. J. Vac. Sci. Technol. A4, 874 (1986).
7. Himpsel, F.J., and Fauster, Th., J. Vac. Sci. Technol. A2, 815 (1984).
8. Gioni, M., Joyce, J.J. and Weaver, J.H., J. Vac. Sci. Technol. A3, 918 (1985); Hughes, G., Ludeke, R., Schäffler, F., and Rieger, D., J. Vac. Sci. Technol. in press.
9. Ludeke, R., Surf. Sci. 168, 290 (1986).
10. Brandt, C.D., Hennel, A.M., Pawlowicz, L.M., Dabkowski, F.P., Lagowski, J. and Gatos, H.C., Appl. Phys. Lett. 47, 607 (1985); Phys. Rev. B33, 7353 (1986).

A Comparative Study of Y and Other Transition Metals on GaAs(110)

F.Schäffler, G.Hughes*, W.Drube, R.Ludeke and F.J.Himpsel

IBM T.J.Watson Research Center, P.O.Box 218, Yorktown Heights, NY 10598, USA

Abstract

Interface chemistry and Schottky-barrier formation of Y/GaAs interfaces are studied by high resolution photoemission (PES) and inverse-photoemission (IPES) spectroscopies and are compared with results from other transition metals on cleaved GaAs surfaces. As with all other transition metals studied so far, the interface chemistry is characterized by a heavily reacted layer, which involves both Ga and As atoms. Ga diffuses into the overlayer, while As stays close to the interface, in contrast to the inverse behavior found in many other transition-metal/GaAs systems. Contrary to e.g. Ti or V, the PES and IPES spectra of Y overlayers show at low coverages no d-electron related filled or empty states in the bandgap of GaAs. The direct involvement of rehybridized d-electron states in the Fermi-level pinning, that has been proposed for several other transition metals, can be ruled out at least for the Y/p-GaAs interface. Alternative mechanisms responsible for the observed Schottky-barrier are discussed. The variation of the barrier height with coverage indicates an influence of the metallic properties of the overlayer on the final Fermi-level pinning position. This applies especially for n-GaAs, for which the final barrier height is not established before the overlayer reaches a thickness of $\geq 10\text{\AA}$. The variation of the band bending with coverage suggest a change in the energetic distribution of acceptor states with increasing Y-coverage.

1. Introduction

The characterization of the microscopic mechanisms leading to the formation of Schottky-barriers on III-V semiconductors has always suffered from a lack of sensitivity both at low metal coverages, for which the density of interface states necessary for Fermi-level pinning is only of the order of 10^{12} cm⁻², and at higher coverages, for which the metal conduction band overlaps the semiconductor valence band and part of the intrinsic bandgap. Consequently, photoemission experiments (PES) were until recently not able to provide spectroscopic evidence for these bandgap states and their energetic distribution. Therefore, all models proposed for the Schottky-barrier formation mechanism are either based on theoretical results ⁽¹⁾⁻⁽⁴⁾, or on the interpretation of indirect experiments ⁽⁵⁾⁻⁽⁷⁾. An example of the latter is the variation of the Fermi-level pinning position within the bandgap as a function of adsorbate coverage, which can usually be fitted by one pair of effective donor and acceptor levels, but with a substantial ambiguity in their respective energy levels. ⁽⁸⁾ Novel techniques ^{(9),(10)} will most likely play an important role in direct spectroscopy of interface states in the near future, but at present, only limited data are available. Another approach was recently chosen by Ludeke *et al.* ^{(11),(12)} who studied transition metals on cleaved III-V semiconductor surfaces with conventional PES techniques. These experiments were based on the relatively large scattering cross-section of d-electrons and the fact that several transition metals have been identified as deep traps in the bulk of both group IV and III-V semiconductors. The latter aspect is of substantial technological importance, (e.g. Cr or V doping of GaAs in the production of semi-insulating substrate material), and has led to a large variety of theoretical ^{(13),(14)} and experimental ⁽¹⁵⁾⁻⁽¹⁷⁾ papers on that subject. Therefore, it is well known that a transition metal impurity usually substitutes a group III atom (cation) in a III-V semiconductor lattice, which causes a rehybridization of the d-electrons. The tetrahedral crystal field leads to a splitting of the d-band into bonding and empty or partly

filled antibonding and nonbonding levels. Depending on the energetic position of these levels with respect to the intrinsic bandgap and on the charge state of the substitutional impurity, such a state can act as donor and/or acceptor. Little is known so far about possible corrections for these energy states as the impurity is moved to the surface or to a metal/semiconductor interface, which reduces the symmetry of the problem. However, since the precision of theoretically predicted impurity levels is of the order of the bandgap itself, present theories are at best capable of giving chemical trends rather than predicting reliable absolute energy values. In addition, the reactivity of most of the transition metals suggests that not only substitutional cation defects but also more complicated defect complexes are created when evaporating transition metals on clean semiconductor surfaces. Hence, it appears necessary to study several transition metal/semiconductor interfaces individually with the aim of establishing chemical trends for their relevance in the Schottky-barrier formation process.

So far, detailed Schottky-barrier studies have been published for Ti($3d^24s^2$ configuration), Pd($4d^{10}5s^2$), V($3d^34s^2$), and Mn($3d^54s^2$) on n- and p-type GaAs^{(11),(12)}, with the latter two metals also reported on InP⁽¹⁸⁾. In all these systems d-electron related emission was observed in the intrinsic semiconductor bandgap up to the Fermi-level for coverages well below the formation of a metallic overlayer. This finding provides strong evidence for the direct involvement of transition metal impurities in the Schottky-barrier formation mechanism and was recently supported by inverse photoemission results for some of these interfaces, which showed empty states in the bandgap down to the Fermi level^{(19),(20)}. All four transition metals mentioned have more than three valence electrons, which means that they can act - in principle - as donor and acceptor states, since the neutral charge state at a substitutional cation site is $3+$. In the following, we present PES and IPES (inverse PES) results of Y on GaAs, which is particularly interesting, since the $4d^15s^2$ configuration of Y is not expected to

produce a donor state at a substitutional cation site, as all three valence electrons are involved in the chemical bonding. The differences in chemistry and Fermi-level pinning are illustrated by comparing these results with experiments of other transition-metal interfaces.

2. Photoemission and Inverse Photoemission Experiments

All PES experiments were performed at the VUV ring of the National Synchrotron Light Source in Brookhaven, NY. The 6m toroidal grating monochromator and the 2D display analyzer, which was used in an angle integrating mode, have been described elsewhere ⁽²¹⁾. Normal emission IPES measurements were performed in a special spectrometer using a grating monochromator and multichannel detection of the photon spectrum ⁽²²⁾. GaAs single crystals with a Si (n-type) doping concentrations of $2 \cdot 10^{17} \text{ cm}^{-3}$, and Zn (p-type) doping of $5 - 10 \cdot 10^{17} \text{ cm}^{-3}$ were pre-oriented and cut in bars of $3 \times 3 \text{ mm}^2$ cross-section in the (110) cleavage plain. The samples were cleaved *in situ* and tested for flatband condition; only cleaves with an initial band bending of less than 150mV were used for further experiments. High purity Y was evaporated from Y ribbons, which were heated by an electron-beam or direct resistive heating. After careful outgasing of the sources, the system pressure could be kept in the middle 10^{-10} Torr range during evaporation, up from a base-pressure of $\approx 10^{-10}$ Torr. Evaporation rates were calibrated with a quartz crystal monitor and checked before and after each evaporation. Rates were adjusted between 10^{-3} and $5 \cdot 10^{-2} \text{ \AA}/\text{sec}$, with the higher ones used at coverages exceeding 1 \AA . All evaporations and measurements were carried out with the cleaved sample held at room temperature. Coverages are given in units of Ångströms, with an equivalent monolayer (defined as $8.85 \cdot 10^{14} \text{ atoms}/\text{cm}^2$, the atomic density of a GaAs (110) layer) of Y, V, Ti, Pd corresponding to a thickness of 2.95, 1.26, 1.56, 1.30 \AA , respectively. Note that an equivalent ML of Y is up to two times thicker than for the other transition metals discussed. Core level spectra were taken in a surface

sensitive mode by choosing appropriate photon-energies to achieve minimal electron escape depths ($\leq 5\text{\AA}$). The bandpass of the analyzer was set to give an estimated combined resolution of monochromator and analyzer of ≤ 200 meV for core level spectra, and ≤ 400 meV for valence band spectra. The energy resolution of the IPES spectra is estimated to be 300meV. The digitally recorded core level spectra were decomposed into their respective spin-orbit-split components by means of a computer routine described in detail elsewhere ⁽²³⁾. In brief, the least square routine minimizes the difference between the actual spectrum and a synthesized one, which is generated from spin-orbit-split Lorentzian doublets broadened by a Gaussian line-shape, the latter accounting for instrumental broadening as well as for inhomogeneities in chemical phase and band bending. The number of adjustable parameters is kept minimal by determining spin-orbit-splitting and the intensity ratio between the spin-orbit-split components from the spectra of the clean sample, and keeping these constant for all coverages and chemically shifted components.

2.1 Interface Chemistry

Fig.1 shows the evolution of the As-3d and Ga-3d core levels as a function of Y coverage. The dots represent the data after subtraction of a smooth background, while the solid lines show the fitted components. The line through the data points is actually the sum of the fitted components and demonstrates the quality of the fits. The spectra of the fresh cleave (labeled "clean") show the well-known decomposition into surface and bulk components ⁽²⁴⁾. The former, which accounts for about 30% of the total core level emission under surface sensitive conditions, results from the charge redistribution in the topmost layer, a consequence of the relaxation of the (110)-surface. Up to a coverage of $\approx 0.3 \text{\AA}$, the spectra are basically only affected by band bending which is identical for both core levels. The spectra in Fig.1 are from an n-type sample, the band bending shift is therefore directed towards higher kinetic

energies. In addition, the components are slightly broadened with coverage, which is mainly due to inhomogeneities in band bending at sub-monolayer coverages. For coverages beyond $\approx 0.3 \text{ \AA}$ chemically shifted components become noticeable, which appear on the high kinetic energy side of both bulk components. This additional component is clearly observed in the Ga-3d spectra and becomes obvious when followed from higher to lower coverages. The chemically shifted component of the As-3d core level is not resolved for coverages lower than a few \AA , as it partly overlaps the surface component, which appears, in contrast to the Ga-3d signal, on the high kinetic energy side of the bulk signal. The existence of a superimposed, chemically shifted component is nevertheless noticeable from both the broadening of what seems to be the As-3d surface component, which is not observed to that extent in the Ga-3d spectra, and from its absolute increase in integrated intensity, which is not expected for a pure surface component. With increasing coverage both core levels show increasing signal from the reacted components, which steadily shift to higher kinetic energies. For a coverage of about 5 \AA coverage (corresponding to $\approx 2\text{ML}$), the reacted components are of comparable intensity to the bulk signals, but dominate the spectra at 10 \AA , the largest coverage for which the bulk components could be resolved. Beyond 10 \AA (see Fig.2), the As-3d signal is stronger attenuated than the Ga-3d signal, the latter still being present at a coverage of 35 \AA . At this value the As-3d signal is just noticeable.

Additional information on the chemical surrounding of the reacted species can be derived from the lineshape of these signals: At coverages $\geq 1 \text{ \AA}$, the reacted Ga-3d signal shows a pronounced asymmetry with a low energy tail, which is indicative of many-body effects in the photoemission process, resulting from the dilution of Ga atoms or small Ga clusters in a metal environment ⁽¹¹⁾. Such asymmetries are well known from XPS-spectra of metals ⁽²⁵⁾, and can to a good approximation be described by the analytical lineshape given by Doniach and Sunjic (DS) ⁽²⁶⁾, which was used in our fits for the chemically shifted Ga-3d component.

The shifted As-3d component, on the other hand, shows only a minor, if any, asymmetry (compare the two spectra at 10Å coverage in Fig.1). This finding together with the fact that the As-3d signal is more rapidly attenuated with increasing coverage suggests that reacted As atoms stay close to the interface in a predominately covalent or ionic local bonding environment, while Ga atoms diffuse into the growing Y film. Thus, the electron-hole pair creation near the Fermi-edge, which is possible in a metallic environment and responsible for the DS-line-shape, is strongly suppressed in the case of the reacted As component, in sharp contrast to the core level signals of Ga atoms (or of small Ga clusters) diluted in the Y host. Besides the different line shape of the reacted components, the FWHM is in both cases very broad compared to the bulk signals. This broadening indicates a variety of different local chemical environments with slightly different binding energies, which can not be resolved in the spectra and consequently appear as an increase of the Gaussian linewidth in our fitting routine. Such a strongly interacted layer is typical for the first few layers of transition metals on GaAs and has also been observed for Pd ⁽¹¹⁾, Ti ^{(11),(27)}, V ^{(12),(28)}, Mn ⁽¹²⁾, Fe ⁽²⁹⁾ and Cr ⁽³⁰⁾. For all these cases one observes at higher coverages, when the supply of semiconductor species is diffusion limited, only one Ga-3d component, while one or two relatively sharp reacted components of the As-3d level survive. This applies also for Y and is illustrated in Fig.2 for coverages of 10 and 35Å. The intensity scale in Fig.2 is identical for all four spectra and shows the strong attenuation of the As-3d signal. This is not the case for the other transition metals mentioned, which are characterized by Ga staying close to the interface and As diffusing into the growing film.

2.2 Fermi-Level Pinning

The spectral decomposition of the Ga-3d and As-3d core levels into bulk, surface and chemically shifted components allows to monitor the Schottky-barrier formation by following the energetic position of the bulk components as a function of coverage. The resulting shift of the Fermi-level at the interface with respect to the valence band maximum (VBM) is plotted in Fig.3 for n- and p-doped samples. The data points represent the relative shifts of the bulk component and are aligned with respect to the VBM, assuming flatband condition for the clean cleaved p-type sample. This results in a starting value of the Fermi-level 70meV above VBM as calculated from the doping of our p-type samples. The assumption of flatband condition for the cleaved p-type sample is justified from comparing many cleaves, which showed that cleavage induced initial band bending affects mainly n-doped samples. Nevertheless, we can not completely rule out a small initial band bending on the p-type sample, which would result in a systematic error in the plotted Fermi-level positions. From comparisons with other cleaves, we estimate this error in the absolute energy values depicted in Fig 3 to be less than 50meV. The precision of the relative changes in the Fermi-level position is limited by the differences between the Ga-3d and As-3d derived band bending. As Fig.3 shows, these differences are smaller than 50meV for all coverages studied, even in the range beyond 1\AA , where the chemically shifted component complicates the Ga-3d spectra. This demonstrates that our fitting procedure is capable of separating the true bulk components with high precision, even in the case of a strongly interacted interface. Nevertheless, it has to be pointed out that the reaction products limit the maximum coverage for which the bulk component can be reliably extracted from the spectra to $\leq 10\text{\AA}$ ($\approx 3\text{ML}$). Similar limits have been found for other transition metals ^{(11),(12)}, and appear to be typical for reacted overlayers, which do not show any tendency for clustering or island growth. The absence of cluster

growth is clearly demonstrated by the small effective electron escape depth: From the attenuation of the Ga-3d and As-3d bulk components as a function of Y-coverage, we derive a escape depth of $3 \pm 0.5 \text{ \AA}$ in surface sensitive condition, which is comparable to the $2 \pm 0.5 \text{ \AA}$ found for Ti overlayers ⁽¹¹⁾.

The variation of the Fermi-level pinning position as a function of Y coverages reveals a pronounced asymmetry between n- and p-type samples: While the Fermi-level shift at the p-type sample shows a relatively abrupt increase to within 100meV of the final value in the coverage range between 0.01 and 0.1 \AA , the n-type sample is characterized by a gradual shift over the entire, experimentally accessible coverage range. At 10 \AA both samples reach the same pinning position in the band gap. Though the Fermi-level shift on n-GaAs does not show a clear saturation behavior by then, we expect only minor changes at higher coverages once a metallic overlayer is formed, especially for the strongly reactive transition metals, which show no indication for clustering or island growth, as mentioned before. The latter growth mode is important for non-reactive systems like Ag on GaAs, where changes in the pinning position have been observed for coverages $\geq 20\text{ML}$ (Ref. 23, 31). However, the delayed pinning in such cases is attributed to lateral inhomogeneities in coverage (and consequently in pinning) rather than to intrinsic changes in the interface states ⁽²³⁾.

Although there may be small additional changes in Schottky-barrier height at higher coverages, which would require other techniques to be detected, the values reached within the coverage range accessible by PES experiments already allow a comparison between different transition metal overlayers. For that purpose we marked on the right hand ordinate in Fig 3 the Fermi-level pinning positions for several transition metals reached at comparable coverages. These pinning positions, which are spread over a range of about 300meV within

the bandgap, are discussed together with the apparent differences in interface chemistry in section 3.

2.2 Valence Band Studies

In addition to core level studies, which give information about the interface chemistry and the band bending, we also performed valence band studies of filled and empty states to obtain further insight into the possible Schottky-barrier formation processes. Fig. 4 shows valence band photoemission spectra of an n-GaAs sample for several Y coverages at a photon energy of 90eV. The abscissa is scaled in energy relative to the Fermi level, i.e. the raw data in the left panel show the changes in valence band emission including the band bending shift. The intensities for the different coverages are not to scale so as to reveal details at low coverages. The raw data are complemented by difference spectra on the right hand side, which depict the spectra at the indicated coverages after subtraction of the clean spectrum. For this purpose, the two respective spectra have been corrected by the band bending shift derived from the substrate core level signals and aligned in intensity by scaling to the low-energy feature in the valence band. The scaling works quite well for Y coverages below 1 \AA , but the raw data in the left panel indicate a shift of the lowest valence band peak towards higher energies, which makes a proper alignment somewhat ambiguous at higher coverages. The observed shift itself is not unexpected, since the lowest valence band peak is mainly derived from As-4s orbitals and is therefore strongly affected by the presence of a reacted As species at the interface. Consequently, the shift of that peak follows closely the energetic position of the reacted As-3d component (compare Fig. 1).

The raw data, and more clearly the difference spectra, show emission from the Y-4d level for coverages as low as 0.1\AA (0.03ML), which appears around 7eV below the Fermi level, developing successively to the dominating valence band feature with increasing coverage. An additional peak appears in the difference spectra at $\approx 11\text{eV}$ below E_f , which results from the mentioned shift of the As-4s derived valence band feature. The topmost spectrum at $\approx 35\text{\AA}$ is characteristic for metallic Y and shows in the enlarged section the Fermi-edge, made up predominately from s-electrons. There is no indication either in the raw data or in the difference spectra for additional emission in the band gap region up to coverages of several \AA , at which value the Fermi-edge of the truly metallic overlayer becomes observable.

The variations in the density profile of empty states above E_f as a function of Y coverage are shown in Fig.5. The IPES spectra were taken in normal emission ($k_{\parallel} = 0$) at an electron energy of 15.3eV. The raw data in the left panel are normalized to the electron flux; the right panel shows difference spectra between the respective spectrum at the indicated coverage and the clean spectrum. The evolution of the raw data, and more pronounced the difference spectra, show the development of the empty d-states as a broad peak at 4eV above E_f . The other major change is the disappearance of the relatively sharp feature at the conduction band onset of the clean surface, which is attributed to a surface state. This effect becomes visible in the difference spectra as a dip around 2eV, and partly obscures the tail of the d-related signal that extends into the bandgap with increasing coverage. This tail is clearly visible at the two highest coverages studied. The final spectrum at 28\AA ($\approx 10\text{ML}$) shows a distinct cut-off at the position of the Fermi-level, indicating that the Y-overlayer has bulk character by then. Nevertheless, the spectra do not show evidence for empty states in the bandgap for coverages below 2\AA .

It is obvious from the PES and IPES experiments that the filled and empty states created by the Y d-levels do not overlap the intrinsic bandgap region of GaAs at low coverages, but appear several eV inside the valence and conduction band, respectively. Emission within the bandgap becomes visible after the overlayer has metallic character. This behavior is substantially different from other transition metals studied recently, which show filled and empty states within the bandgap at coverages much below one monolayer, i.e. before the overlayer can develop metallic properties. This is demonstrated in Fig.6, which depicts the additional filled and empty states in the vicinity of the bandgap induced by small amounts of Ti, V and Pd deposited on cleaved GaAs samples (solid lines). The dashed curves show the valence and conduction bands as derived from PES and IPES experiments on clean cleaves. The d-derived bandgap states extend in all three cases up to the Fermi-level, providing strong evidence for their direct involvement in the pinning process.

3. Discussion

The experimental results presented in the preceding section, reveal pronounced differences in the chemical and electronic behavior of Y on GaAs with respect to other 3d- and 4d- transition metals. As far as chemistry is concerned, the predominant outdiffusion of Ga rather than As into the metal overlayer has not been observed for the 3d- and 4d-transition metals studied so far. The lineshape of the reacted As-3d compound indicates a strong bond between As and Y atoms, which is consistent with the large electronegativity difference of the two species: Y has, with a value of 1.2 (Ref.32), the lowest electronegativity of all 3d- and 4d-transition-metals, which is substantially lower than that of As (2.0) and also less than the value for Ga (1.5). In contrast, the other transition metals that have been studied (V, Ti, Cr, Mn, Fe, and Pd) have electronegativities comparable to that of Ge. This suggests that

the interface reactions consist basically in the formation of Y-As bonds, which releases Ga-atoms from their lattice sites. The reaction at this stage is not stoichiometric, as can be seen in the inhomogeneous broadening of the reacted Ga and As corelevels, and most likely affects several atomic layers of the substrate. The observed shift of the reacted As-3d component toward higher kinetic energy results from a charge transfer from Y-atoms, as expected from the large electronegativity difference. This effect becomes also visible in the shift of the As-4s derived valence band feature that has been mentioned above (see Fig.4). The Ga-atoms released in the earlier stages of the interface reaction diffuse into the Y-overlayer, probably forming an alloy, which becomes more and more Y-rich with increasing thickness of the overlayer, as the interacted layer forms an effective barrier for further out-diffusion of Ga-atoms. The final stage is reached when isolated Ga-atoms are surrounded by a local Y-environment, resulting in a Ga-3d spectrum consisting of only one sharp peak (see Fig.2).

The simplified description of the likely chemical reactions at the Y/GaAs interface is based on the observed changes in the core level spectra and the differences in electronegativity. The use of electronegativity arguments seems to be justified for the present case, and is supported by recent experiments at the interface between the 4f-metal Yb and GaAs: ⁽³³⁾ Yb has a comparable small electronegativity of 1.1, and shows a similar reaction kinetic at the interface as Y, i.e., Ga diffuses into the overlayer while As stays close to the interface. On the other hand, care has to be taken when the electronegativity differences between the reacting species are small, as is the case with most other transition metals on GaAs: Although a cation replacement reaction is the most probable initial reaction for all of these interfaces, it is at present not understood, why for those systems the cation stays

close to the interface upon further metal deposition, while the anion diffuses into the overlayer.

The other interesting aspect of the Y/GaAs system, namely the electronic properties of the interface, differs also substantially from the behavior found with other transition-metal/GaAs interfaces: From the simple counting of the valence electrons, mentioned in section 1, it is clear that no d-electron related filled states of Y atoms at a substitutional cation site are expected to overlap the intrinsic bandgap region. This expectation is confirmed by the PES experiments, which are consistent with the assumption of a cation replacement reaction, but also reveal that the filled d-state is located several eV below E_F . Nevertheless, we observe a Schottky barrier of 0.68 ± 0.05 eV on p-type, and of 0.73 ± 0.05 eV on n-type GaAs, close to the barrier heights found with V and Ti overlayers. The latter two metals show a large density of filled and empty, d-electron related states at the Fermi-level at coverages long before the overlayer becomes metallic (see Fig.6). This finding together with the known donor and acceptor properties of these metals in bulk samples led us to the conclusion that the rehybridized d-orbitals provide the dominating mechanism for the observed Schottky-barrier formation.^{(11),(12)} The same argument applies for Pd (Ref.11) and to some extent also for Mn (Ref.12), but the lack of d-electron related bandgap emission in the present case of Y rules out the involvement of d-orbitals in the pinning mechanism for p-type GaAs. The situation is not so clear-cut for n-type GaAs, which is characterized by a gradual shift of the Fermi-level toward the final pinning position: About 40% of the total band bending occurs in a coverage range beyond 0.1 \AA^2 , where chemical reactions and tailing of the predominately d-like empty states into the intrinsic bandgap become visible in the experiments. In contrast, the Fermi-level on p-GaAs lies within 100 meV of the final pinning position already at a coverage of 0.1 \AA^2 . This pronounced asymmetry in

Schottky barrier formation suggests different mechanisms being responsible for the creation and energetic distribution of donor and acceptor states at the Y/GaAs interface. The following discussion will therefore treat the pinning on n- and p-type samples separately.

The p-GaAs/Y interface reaches its final pinning position at very low coverages with only minute changes in the regime of strong chemical reactions at the interface and the eventual development of a metallic overlayer. The results suggest that the energetic distribution of donors created upon deposition of about 0.1 \AA Y is almost unaffected by the subsequent interface chemistry and the screening properties of a true metal overlayer. This implies that either a high density of donors of the order of 10^{14} cm^{-2} has been created at 0.1 \AA coverage, or that the same kind of donor states is also produced in the reaction regime. In either case, it is expected that some 10^{14} cm^{-2} donors are present at several \AA coverage, when the overlayer becomes metallic. Otherwise, the metallic screening properties would affect the final pinning position according to recent theoretical results ^{(34),(35)}.

The experiments do not provide direct access to the origin of the donor states created upon Y-deposition on p-GaAs: As the experiments lack any evidence for filled gap states in the low coverage range, the Y/GaAs interface resembles the situation found for most of the simple, non-transition metals, where surface donor states also escaped detection in photoemission experiments, either because of the small density of those states or, more likely, because of their small photoemission cross section. Nevertheless, the observed interface chemistry and the pinning behavior allow to select some potential mechanisms, which will be briefly discussed in the following.

The reactivity of Y that is observed in the core level spectra and the local inhomogeneities inside the reacted layer, which lead to a broadening of the reacted Ga-3d and As-3d components, suggest that besides substitutional cation impurities other kinds of defects, e.g. vacancies or ternary complexes, are created during the first phase of Y deposition. It is well known from calculations that filled and empty electron levels associated with such defects can be located within the intrinsic gap of GaAs, and therefore can contribute to the Schottky-barrier formation⁽³⁶⁾. These theoretical results were important for the formulation of the so called "unified defect model" (UDM), which attributes the Schottky-barrier formation to an universal pair of GaAs-derived defects that are created during the first steps of metal deposition: Ga and As vacancies, or As_{Ga} and Ga_{As} antisite defects have been named as candidates for donor and acceptor states, respectively^{(37),(38)}. Despite recent modifications that reduce some of the early shortcomings of the UDM,⁽⁵⁾ such as the prediction of two different pinning levels for n- and p-type semiconductors, the main problem remains the experimental identification of the proposed defects. Moreover, the claimed universality of the model has been questioned by recent experiments on the Ge/GaAs interface, which revealed Fermi-level pinning only in the case of an amorphous, but not for an epitaxial Ge overlayer⁽³⁹⁾. This finding is hard to reconcile with the UDM, as it appears unlikely that native GaAs defects should only be created at low-temperature deposition of Ge, which leads to an amorphous overlayer, but not under epitaxial growth conditions. The interpretation given in Ref.39 attributes the pinning behavior for the amorphous overlayer to Ga- and As dangling bonds at the interface that are not saturated by Ge-bonds because of local disorder in the amorphous film. This mechanism is more satisfactory than one based on intrinsic GaAs defects and might also be important for the present case of a heavily reacted overlayer.

Another possible source of interface states is related to the cation replacement reaction, which we identified as the most likely initial reaction upon Y deposition. At submonolayer coverages the released Ga atoms have to stay at the surface, before a part of them can be successively incorporated into the growing Y film during further Y deposition. The early Y-adsorption regime resembles therefore models that have been proposed for low-coverage Al/GaAs interfaces⁽⁴⁰⁾, where a corresponding Al-Ga replacement reaction was assumed. As neither Al nor Y at a cation site of the surface create intrinsic donor states, it is conceivable that the observed band bending in both cases is due to the replaced Ga-atoms. This argument is supported by the fact that the Ga/GaAs interface is also pinned⁽⁴¹⁾. Unfortunately, no high-resolution band bending studies are available for low Ga coverages ($\leq 0.1\text{\AA}$), which would be necessary to test, if a predominant creation of donors at the Y/GaAs interface can be related to an energetically favorable binding site of replaced Ga atoms at the surface, as is suggested by energy-minimization calculations⁽⁴²⁾. At higher coverages, however, the possible similarity between the Y/GaAs and the Ga/GaAs interface is no longer expected. Ga (like other column III atoms) clusters at room temperature, an effect which is unlikely in the present case because of the relatively small amount of Ga-atoms released and its alloy formation with the Y overlayer. Hence, the experimental finding that Ga pins both n- and p-GaAs at coverages $> 1\text{\AA}$ (Ref. 41) does not rule out the possibility of a predominant donor creation at submonolayer coverage. Certainly, additional experiments of the Ga/GaAs interface, preferentially performed at low temperatures in order to suppress cluster formation, are necessary to substantiate the relevance of this pinning mechanism.

As mentioned above, the n-GaAs/Y interface behaves in a substantially different manner as far as Schottky-barrier formation is concerned: Although we observe band bending from

the lowest Y-coverage on, the final barrier height is not established before the overlayer is truly metallic. The gradual shift of the Fermi-level over such a large coverage range has so far only be observed for metal-overlayers that form clusters or islands upon room temperature deposition. Such a growth mode definitely does not apply to the Y/GaAs interface (compare section 2.2). A simple interpretation in terms of lateral inhomogeneous band bending is therefore inadequate for the present system, especially as p-GaAs would be affected as well, which is obviously not the case. The n-GaAs/Y interface appears to be much more complicated and most likely has several pinning mechanisms involved. At low coverages donor as well as acceptor states are produced, since both n- and p-type substrates show band bending from the smallest Y-depositions on. Any of the three mechanisms discussed above as sources for donor creation can in principle also be associated with acceptor production. However, it appears unlikely that the defect mechanism of the UDM is applicable here, as it assumes an acceptor level far down in the bandgap, which does not correspond to the shallow barrier on n-GaAs reached at low coverages. In order to fit the UDM to the Y/GaAs interface, one has to assume that the density of acceptors is too small to pin the Fermi-level at low coverages. This means that the rate for acceptor production would have to be much smaller than the one for donors, which is not supported by experiments on other systems that have been described in terms of the UDM. The second mechanism, namely the donor and acceptor properties of unsaturated dangling bonds at the interface is based on n-GaAs/Ge interfaces only⁽³⁸⁾ and needs confirmation on p-type substrates before its relevance for the present interface can be judged. More experiments are also necessary for the third proposed mechanism, which is related to the role of released Ga atoms at the interface. It is however worth noting that energy-minimization calculations show several energetically favorable binding sites of Ga atoms on the GaAs(110) surface, which differ somewhat in binding energy⁽⁴¹⁾. These sites affect also the associated density of states in the bandgap, i.e.

they can have donor- or acceptor properties. The energy difference between two such sites would then determine the probability of their occupation by released Ga-atoms and might account for a much smaller density of acceptors, which is too low to pin the Fermi-level at submonolayer coverages. In addition, the simple acceptor state might be close to the conduction band, accounting for the shallow barrier found at low coverages at the n-GaAs/Y interface.

Whatever the acceptor-creating mechanisms at low coverages are, the delayed formation of the Schottky-barrier suggests that other mechanisms contribute in the interaction regime. From the low-coverage IPES spectra, we can exclude that empty d-derived states associated most likely with a cation replacement reaction provide a source for acceptors, since such states appear several eV in the conduction band. With increasing coverage, however, the overlayer gradually develops a metallic bandstructure, which is characterized by tailing of the empty states towards the Fermi-level. Although such a tailing does not become obvious in the IPES spectra at Y-coverages below 2\AA , an earlier onset of a gradual overlap between the metal density of states and the semiconductor bandgap appears plausible: A small density of states would most likely escape experimental detection, as the scattering cross section for d-like states at an electron energy of 15.3eV used in the IPES measurements is much smaller than the one in the PES experiments, which were performed at a photon energy of 90eV. Another problem is the disappearance of a pronounced surface resonance in the IPES spectra, which affects the conduction band onset of the clean spectrum. This leads to the negative peak in the difference spectra of Fig.5, which could easily disguise an early tailing of the empty d-states into the intrinsic bandgap.

The gradual development of metal-derived states, which move downwards with increasing coverage, could provide a source for acceptor-like density of states that changes its energetic position with increasing overlayer thickness. Such a mechanism appears interesting, especially in connection with a class of models, which are based on metal-induced-gap states (MIGS) as a potential source for Fermi-level pinning ⁽¹⁾⁻⁽⁴⁾. Such models are usually calculated for abrupt interfaces between semiconductors and metallic overlayers, but it is clear that the metal bandstructure develops gradually under experimental conditions. Nevertheless, it appears impossible, to extract such an effect in a quantitative way from our experiments, since we can not entirely rule out the generation of localized acceptor states at lower energies in the interaction regime, which could as well account for the observed gradual shift of the Fermi-level. Hence, lacking an experimental technique that provides information about the exact distribution of acceptor- and donor-states in the bandgap as a function of coverage, we can only speculate about the potential influence of MIGS. However, it should be pointed out that even if MIGS play a role in pinning the Fermi-level at the n-GaAs/Y interface, their efficiency is obviously very limited and their effect can easily be overruled by a high density of localized interface states: This is observed for the p-GaAs/Y interface as well as for the transition metals in Fig.6, which all show pinning close to the saturation value at very low coverages.

In summary, we have studied the Y/GaAs interface, which shows several unusual features as compared to other transition-metal/GaAs systems. Though the interface is heavily reacted, like with other 3d- and 4d-metals, the small electronegativity of Y compared to Ga and As leads to a strong bond between As and Y and drives substituted Ga atoms into the growing metal film. In contrast, other transition metals studied recently reveal a more com-

plex interface chemistry, which is most likely also started by Ga substitution, but subsequently results in outdiffusion of As into the overlayer.

Besides the interface chemistry, the most remarkable finding is the Schottky-barrier formation, especially the pronounced differences between n- and p-type GaAs: p-GaAs is characterized by Fermi-level pinning at submonolayer coverages, while the Schottky-barrier formation on n-GaAs extends into a coverage range where the overlayer becomes metallic. This means that at low coverages mainly donor-states are created at the interface, while the density or the initial energetic distribution of acceptor states is not sufficient to pin the Fermi-level at its final position. The origin of the surface-donors is not understood yet, but we can rule out that rehybridized d-electrons, which most likely provide donor-states in several other transition-metal/GaAs systems, are involved in the Fermi-level pinning at the Y/p-GaAs interface. Empty d-derived states might play a role as acceptor states in the intermediate coverage regime, but this effect, if it exists, results from the properties of the Y-overlayer and not from the empty levels associated with a simple substitutional defect.

The results of the Y/GaAs interface show that we are still far from understanding the basic, microscopic mechanisms that lead to the formation of a Schottky-barrier. The future development in this field will strongly depend on new spectroscopic methods, which hopefully allow a positive identification of the interface states created at submonolayer coverages, and on the ability for a reasonable description of the intermediate coverage range between interface creation and metallic screening.

4. Acknowledgements

We thank M. Prikas for his expert help in preparing the experiments and the staff of the NSLS in Brookhaven for their technical assistance. This work was partially supported by the U.S. Army Research Office under Contract No. DAAG-29-83-C-0026.

References

* present address: School for Physical Sciences, NIHE, Glasnevin, Dublin 9, Ireland.

1. V.Heine, Phys. Rev. 138A, 1689 (1965)
2. S.G.Louie, M.L.Cohen, Phys. Rev. B13, 2461 (1976)
3. C.Tejedor, F.Flores, E.Louis, J. Phys. C10, 2163 (1977)
4. J.Tersoff, J. Vac. Sci. Technol. B3, 1157 (1985) and references herein
5. W.E.Spicer, T.Kendelewicz, N.Newman, K.K.Chin, I.Lindau, Surf. Sci. 168, 240 (1986) and references herein
6. L.J.Brillson, Surf. Sci Reports 2, 123 (1982) and references herein
7. J.L.Freeouf, J.M.Woodall, Appl. Phys. Lett. 39, 727 (1981)
8. A.Nedoluha, J. Vac. Sci. Technol. 21, 429 (1982)
9. R.Haight, J.Bokor, Phys. Rev. Lett. 56, 2846 (1986)
10. R.E.Vituro, M.L.Slade, L.J.Brillson, Phys. Rev. Lett., 57, 487
11. R.Ludeke, G.Landgren, Phys. Rev. B33, 5526 (1986)
12. G.Hughes, R.Ludeke, F.Schäffler, D.Rieger, J.Vac.Sci.Technol. B4, 924 (1986)
13. H.Katayama-Yoshida, A.Zunger, Phys.Rev. B31, 7877 (1985); Phys.Rev. B33, 2961 (1986)
14. M.J.Caldas, S.K.Figueiredo, F.Fazzio, Phys.Rev. B33, 7102 (1986) and references herein
15. A.M.Hennel, C.D.Brandt, Y.-T.Wu, T.Bryskiewicz, K.Y.Ko, J.Lagowski, H.C. Gatos, Phys.Rev. B33, 7353 (1986)
16. U.Kaufmann, J.Schneider, *Festkörperprobleme, Advances in Solid State Physics*, ed. J.Treusch (Vieweg,Braunschweig 1980) Vol. XX, p. 87
17. B.Clerjaud, J.Phys. C18, 3615 (1985) and references herein

18. F.Schäffler, W.Drube, G.Hughes, R.Ludeke, D.Rieger, F.J. Himpsel, Proc. 10th. Int. Conf. on Solid Surfaces, to be published in J. Vac. Sci. Technol. A (1987)
19. R.Ludeke, D.Straub, F.J.Himpsel, G.Landgren, J.Vac.Sci.Technol. A4, 874 (1986)
20. R.Ludeke, G.Hughes, W.Drube, F.J.Himpsel, F.Schäffler, D.Rieger, D.Straub, G.Landgren, Proc. 18 Int. Conf. Phys. Semicond., to be published
21. D.E.Eastman, J.J.Donelon, N.C.Hien, F.J.Himpsel, Nucl.Instr.Methods 172, 327 (1980); F.J.Himpsel, Y.Jugnet, D.E.Eastman, J.J.Donelon, D.Grimm, G.Landgren, A.Marx, J.F.Morar, C.Oden, R.A.Pollak, J.Schneir, C.A.Crider, Nucl. Instrum. Methods 222, 107 (1984)
22. T.Fauster, D.Straub, J.J.Donelon, D.Grimm, A.Marx, F.J.Himpsel, Rev. Sci. Instrum. 56, 1212 (1985)
23. R.Ludeke, Surf.Sci. 168, 290 (1986)
24. D.E.Eastman, T.-C.Chiang, P.Heimann, F.J.Himpsel, Phys. Rev. Lett. 45, 656 (1980)
25. G.K.Wertheim, P.H.Citrin, *Photoemission in Solids I*, eds. M.Cardona, L.Ley (Springer Verlag, Berlin, 1978)
26. S.Doniach, M.Sunjic, J. Phys. C3, 285 (1970)
27. M.W.Ruckman, M. del Giudice, J.J.Joyce, J.H.Weaver, Phys. Rev. B33, 2191 (1986)
28. M.Grioni, J.J.Joyce, J.H.Weaver, J. Vac. Sci. Technol A3, 918 (1985)
29. M.W.Ruckman, J.J.Joyce, J.H.Weaver, Phys. Rev. B33, 7029 (1986)
30. J.H.Weaver, M.Grioni, J.J.Joyce, Phys. Rev. B31, 5348 (1985)
31. F.Schäffler, G.Abstreiter, J. Vac. Sci. Technol. B3, 1184 (1985)
32. all electronegativity values are taken from W.Gordy, W.J.O.Thomas, J. Chem-Phys. 24, 439 (1955)
33. J.Nogami, M.D.Williams, T.Kendelewicz, I.Lindau, W.E.Spicer, J. Vac. Sci. Technol. A4, 808 (1986)
34. A.Zur, T.C.McGill, D.L.Smith, Phys. Rev. B28, 2060 (1983)

35. C.B.Duke, C.Mailhot, *J. Vac. Sci. Technol.* B3, 1170 (1985)
36. R.E.Allen, J.D.Dow, *Phys. Rev.* B25, 1423 (1982)
37. W.E.Spicer, P.W.Chye, P.R.Skeath, C.Y.Su, I.Lindau, *J. Vac. Sci. Technol.* 16, 1422 (1979)
38. W.E.Spicer, I.Lindau, P.Skeath, C.Y.Su, P.Chye, *Phys. Rev. Lett.* 44, 420 (1980)
39. H.Brugger, F.Schäffler, G.Abstreiter, *Phys. Rev. Lett.* 52, 141, (1984)
40. J.Ihm, J.D.Joannopoulos, *Phys. Rev.* B26, 4429 (1982)
41. P.Skeath, I.Lindau, P.W.Chye, C.Y.Su, W.E.Spicer, *J. Vac. Sci. Technol.* 16, 1143 (1982)
42. D.J.Chadi, R.Z.Bachrach, *J. Vac. Sci. Technol.* 16, 1159 (1982)

Figure Captions

Fig.1 PES spectra of the Ga-3d and As-3d core levels for increasing Y coverage at a photon energy of 90eV. The data (dots) are decomposed into bulk, surface and reacted components. Their sum is represented by the line through the data points. The attenuation of the core level signals with coverage is represented by scaling factors.

Fig.2 Change in the Ga-3d and As-3d core levels between a coverage of 10\AA , which is characteristic for a heavily interacted interface, and a thick Y overlayer. The spectra are to scale and show the much stronger attenuation of the As-3d component compared to the Ga-3d signal. Note that only one sharp Ga-component remains at 35\AA .

Fig.3 Variation of E_F with respect to VBM as a function of Y-coverage. The core level shifts of the Ga-3d as well as of the As-3d bulk-component are plotted. Note the pronounced differences in Fermi-level shift between n-type and p-type samples: While p-GaAs becomes pinned at submonolayer coverages, n-GaAs shows changes in E_F well into the metallic regime of the overlayer. Final pinning positions of other transition-metals on GaAs (Ref.11 and 12) are indicated on the right hand side.

Fig.4 Development of the valence band PES spectra upon Y deposition. In addition to the raw data in the left panel, difference spectra between the spectra at the noted coverages and the clean spectrum are plotted in the right frame. Intensities are not to scale to reveal details at low coverages. The spectrum at 35\AA is typical for an Y-film and shows the mainly s-electron derived Fermi edge in the enlarged section. Additional emission from the Y-d-electron becomes visible from 0.03\AA on and is located about 7eV below E_F .

Fig.5 Normal emission IPES raw and difference spectra for various Y coverages. All spectra are normalized to the electron flux. The appearance of the empty Y-4d states at 4eV above E_f , concomitant with the loss of a surface state at the conduction band onset can be followed down to the lowest Y coverage. The broad 4d signal tails into the bandgap region at coverages above 2\AA , indicating the beginning formation of a metallic overlayer.

Fig.6 In contrast to Y, other transition metals show filled and empty d-electron related states in the bandgap at coverages well below the onset of metallic properties. Ti, V and Pd data are shown as examples. The plots combine photoemission and inverse-photoemission spectra of clean samples (dashed) and difference spectra at coverages of 0.2\AA of the respective metal.

Y on n-GaAs

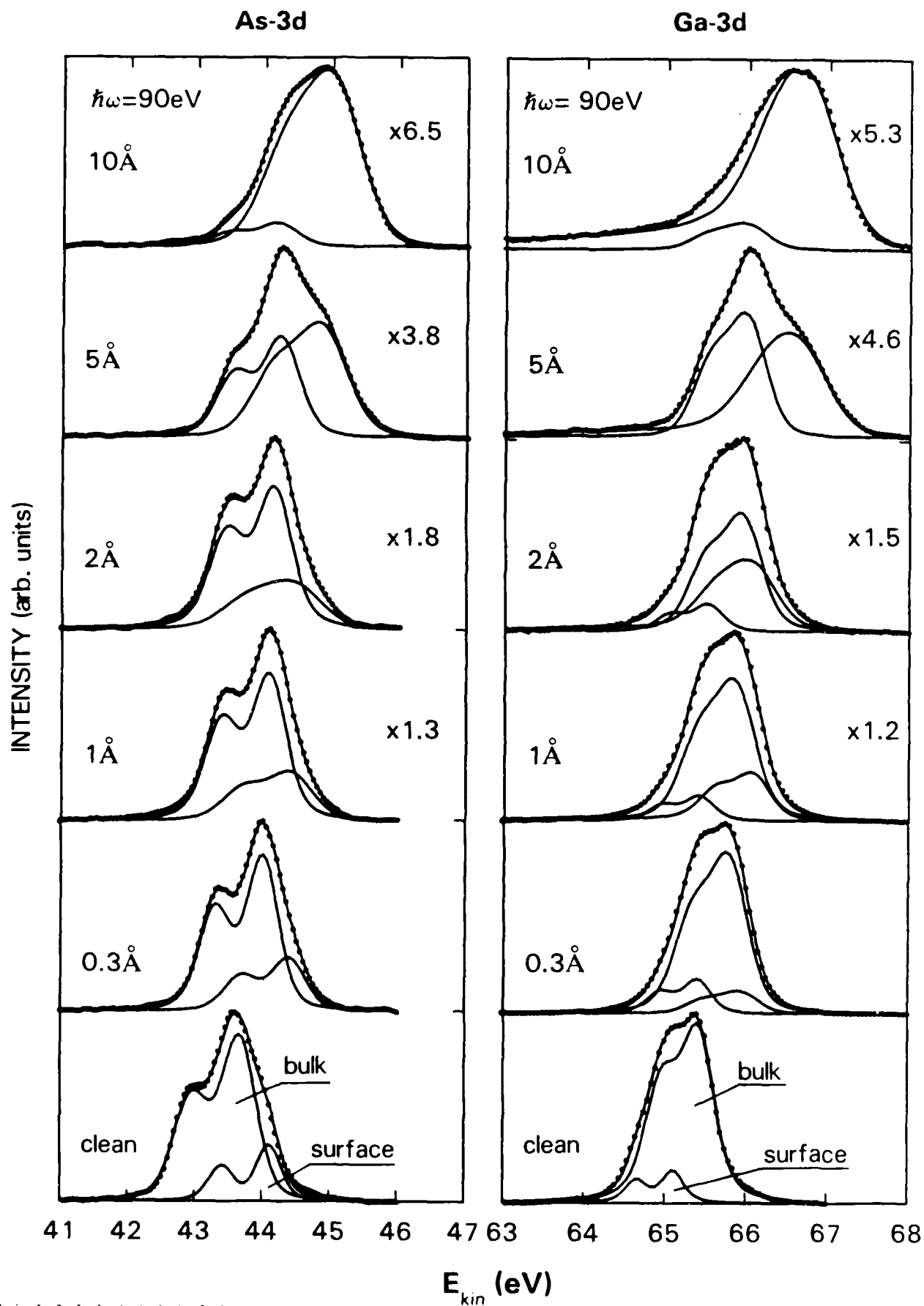


Fig. 1

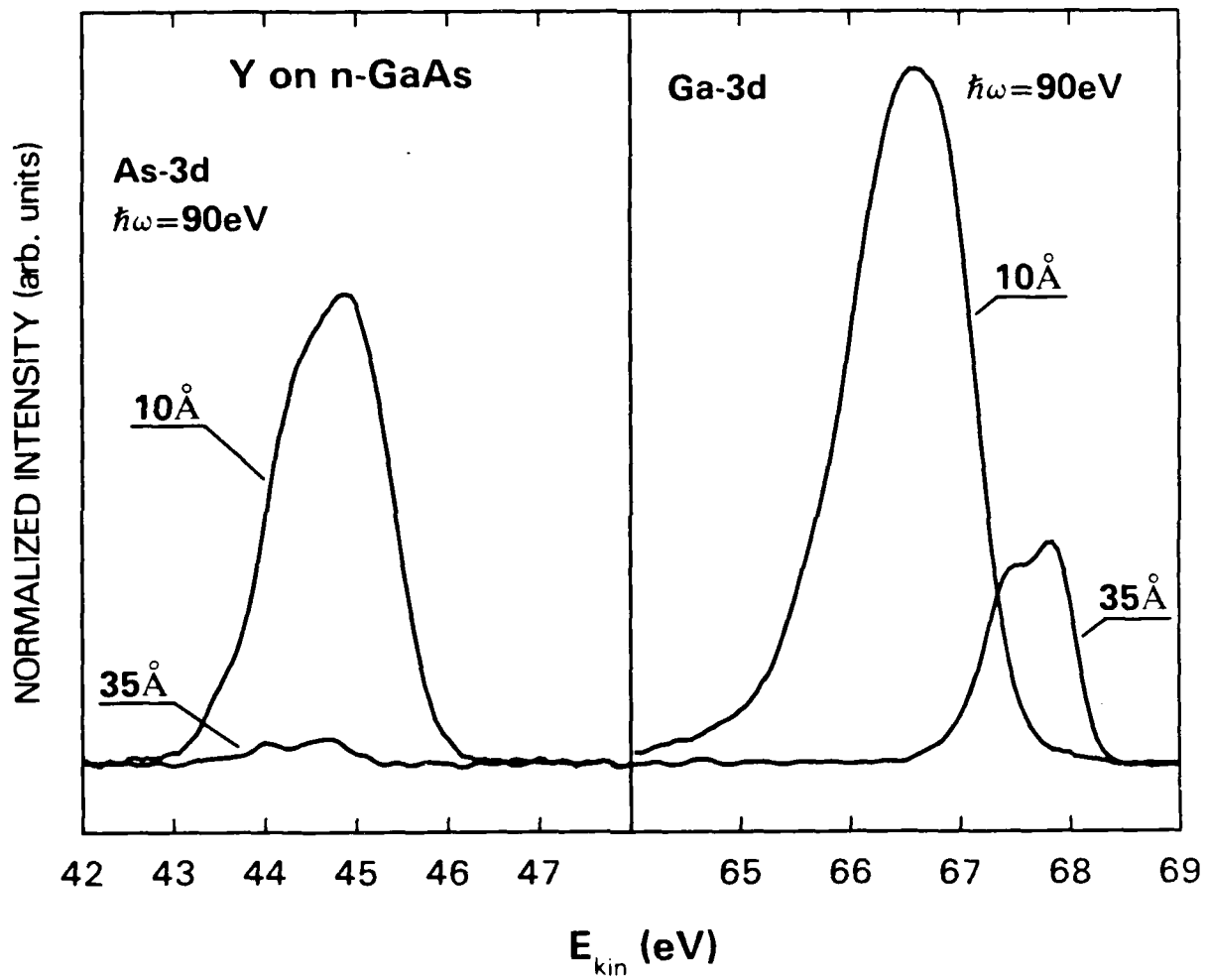


Fig. 2

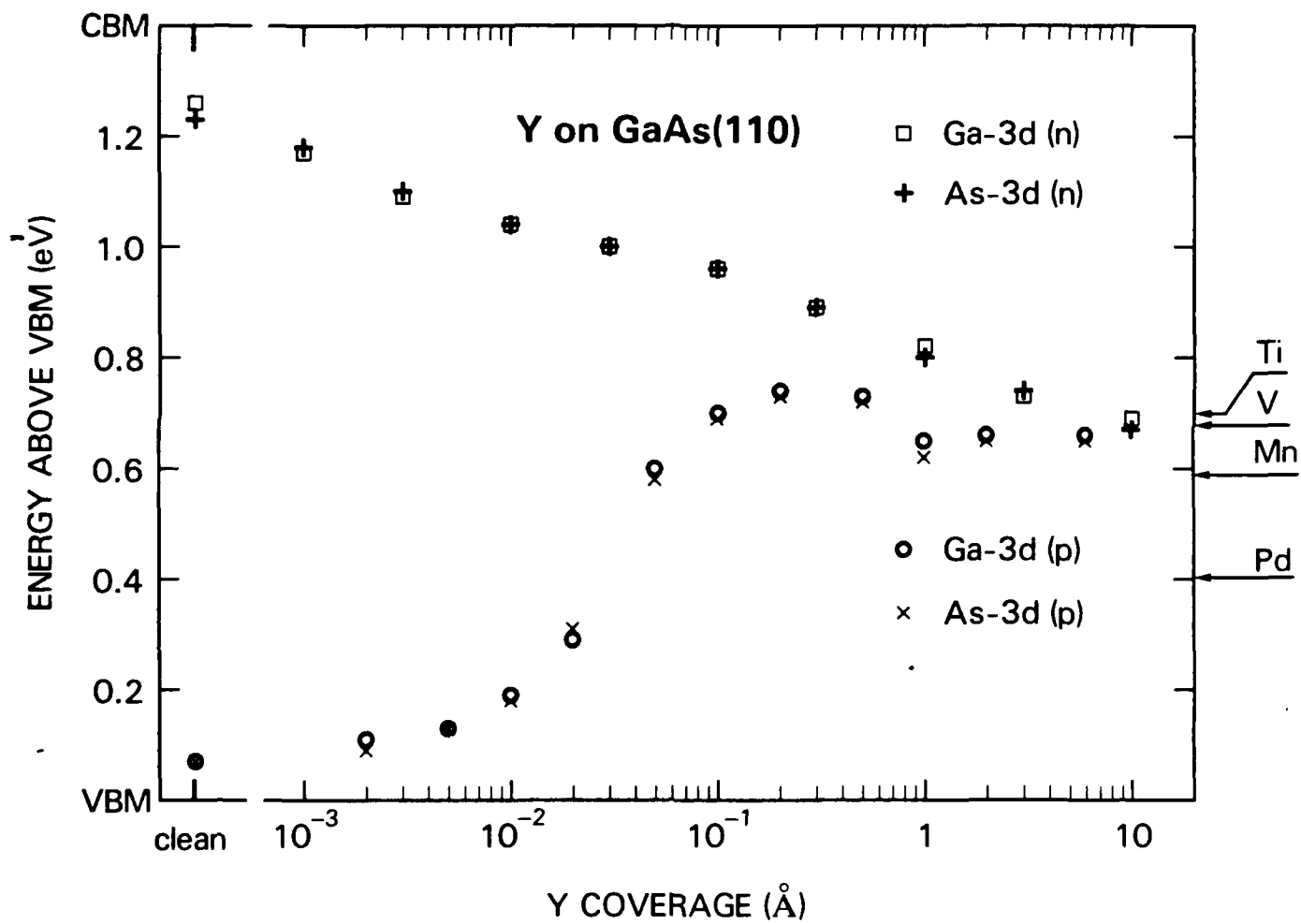


Fig. 3

Y on n-GaAs

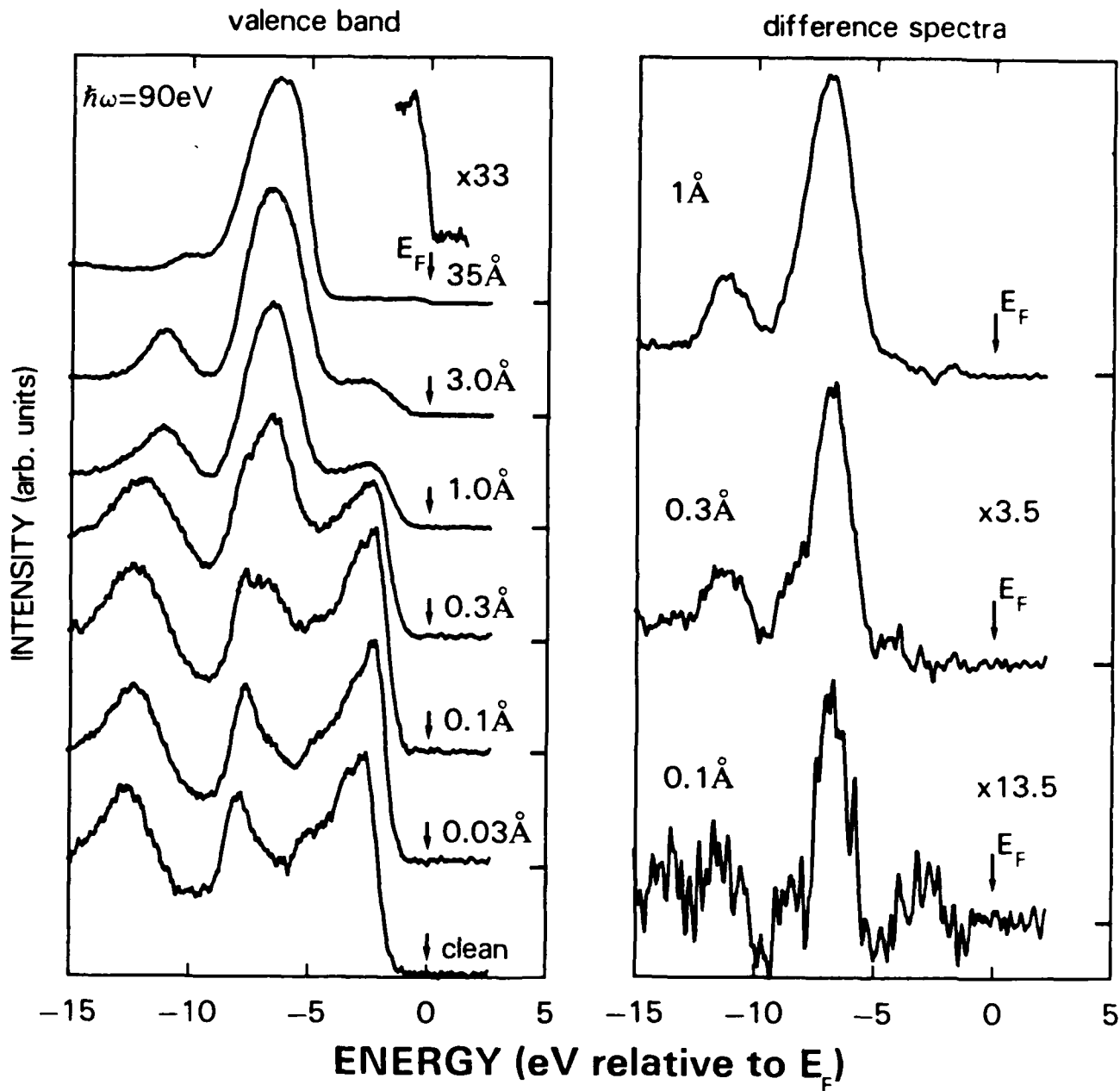


Fig. 4

Y on p-GaAs

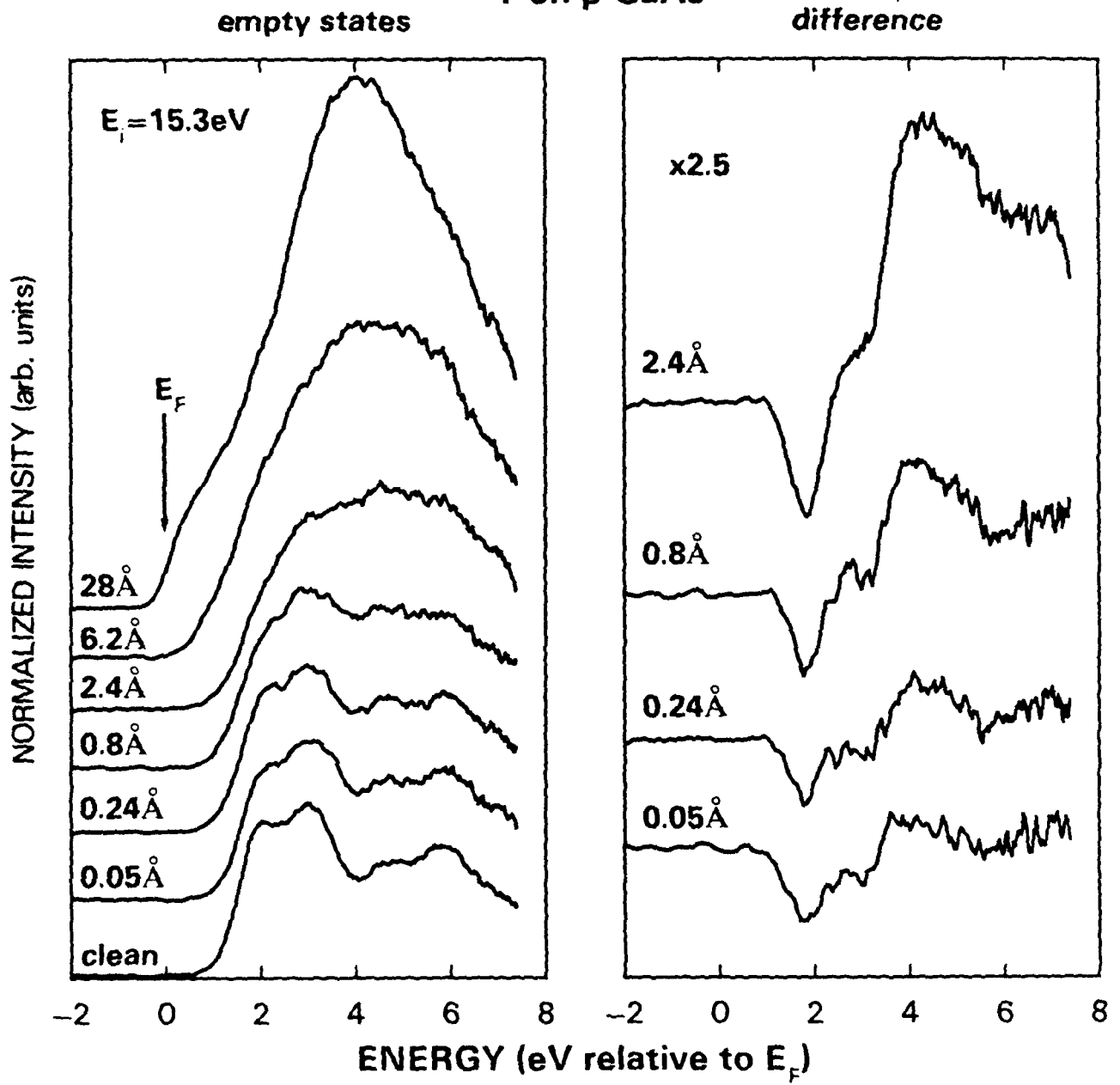


Fig. 5

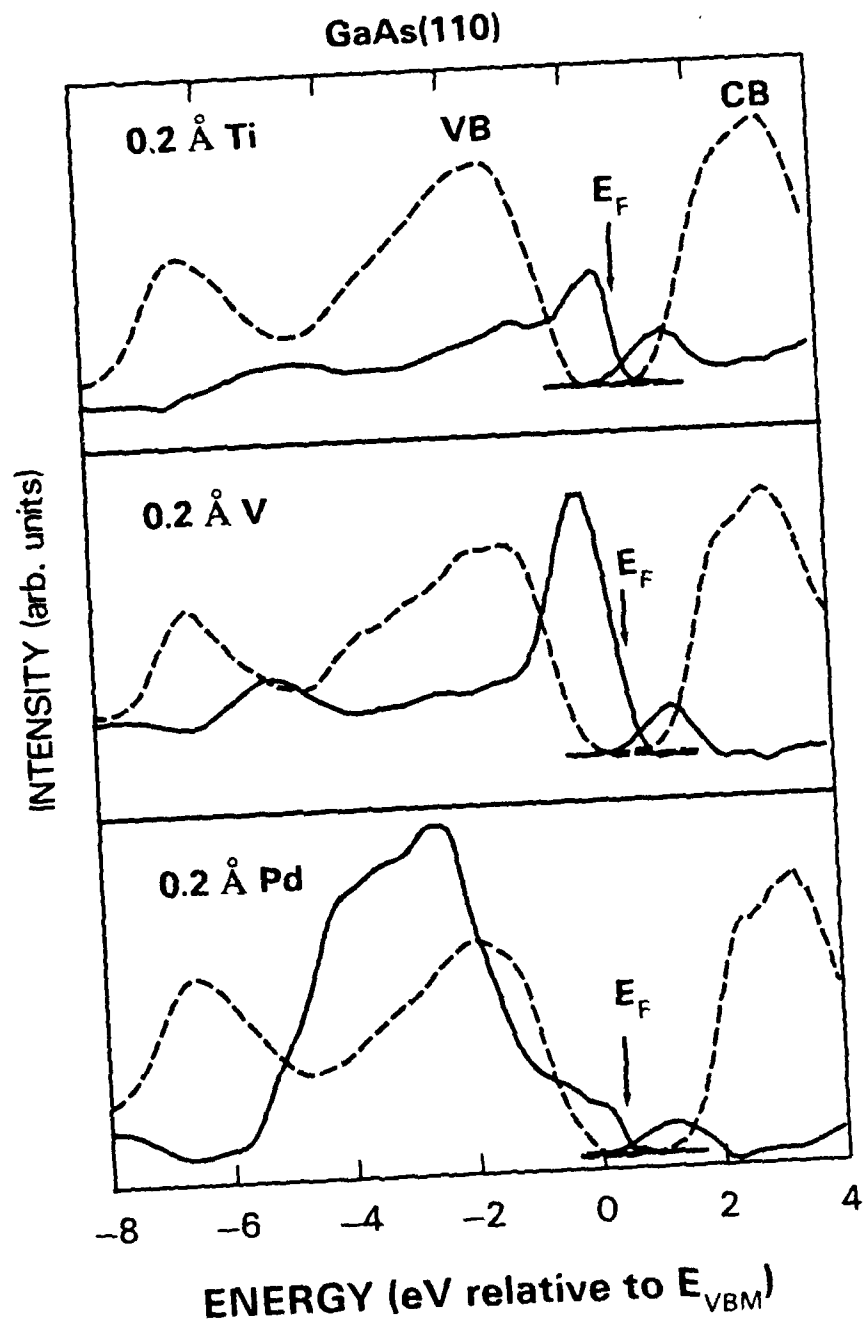


Fig. 6

The Sb/GaAs(110) Interface: A Re-evaluation

F. Schäffler*, R. Ludeke, A. Taleb-Ibrahimi, G. Hughes- and D. Rieger*

IBM T.J. Watson Laboratory, P.O. Box 218, Yorktown Heights, NY 10598

Abstract

The influence of thermal annealing of Sb/GaAs(110) interfaces is studied *in situ* by high resolution photoemission spectroscopy. A detailed lineshape analysis of the Sb-4d core level spectra shows that Sb-deposition at room temperature (RT) does not lead to perfectly ordered growth of the first monolayer (ML), as was assumed so far. Annealing at 330°C results in a highly ordered overlayer that is desorption limited to 1ML. The degree of order affects the barrier height at the interface drastically: While RT-deposition pins the Fermi-level 0.6eV above VBM for p-GaAs, we find a reduction in the band bending by a factor of two after annealing.

PACS Nrs. 68.55.Rt, 73.30.+y, 73.20.At

The Sb/GaAs(110) interface attracted several experimental and theoretical groups because of the epitaxial growth mode of the first Sb layer. Extensive LEED profile analysis showed that the first monolayer (ML) of Sb closely resembles the topmost layer of the relaxed GaAs(110) surface ^{(1),(2)}. Epitaxial Sb-growth is limited to the first ML, followed by three dimensional (3D) cluster growth (Stranski-Krastanov growth). Thermal desorption experiments revealed stability of the first ML up to temperatures of $\approx 550^{\circ}\text{C}$, while Sb in excess of 1ML desorbs already at $\approx 250^{\circ}\text{C}$ ⁽³⁾. The electronic structure of the ordered Sb ML on GaAs(110) has been calculated by two groups ^{(4),(5)}. Both find the filled Sb-derived states below the (Γ -point) valence band maximum (VBM), while the empty states are located above the conduction band minimum (CBM) in the results of Ref.5, but slightly below the CBM in those of Ref.4. The model calculations imply that a ML of Sb should not affect the flatband condition at the surface of clean cleaved p-GaAs, but might result in a small Schottky-barrier on n-GaAs. However, the few band bending measurements published so far are in gross disagreement with respect to each other: Schottky-barriers of $\approx 0.6\text{eV}$ for both n- and p-type GaAs were derived from work function measurements ⁽⁶⁾, while surface-photo-voltage (SPV) experiments indicate that an initial barrier created by a submonolayer coverage of Sb on n-GaAs is largely removed at a coverage of 1 ML and above ⁽⁷⁾. Raman experiments confirm the former results, but show additional changes at the interface for coverages exceeding several ML ⁽⁸⁾. Angle resolved photoemission experiments (ARPES) on cleaved n-GaAs surfaces covered with 1 ML of Sb seem to show good agreement with theory at least for the highest filled surface states ⁽⁹⁾, which were found to lie below the VBM. However, the absolute energetic position of the surface states with respect to VBM appears questionable, as the authors did not determine the band bending independently.

but rather used a literature value of 0.6eV. A smaller value, as is suggested by the SPV results, would shift the filled surface states into the intrinsic band gap and thus could account for a Schottky-barrier on p-GaAs.

The samples for the mentioned LEED and band bending measurements were prepared at room temperature (RT), which was considered sufficient for the growth of an ordered Sb ML. Since Sb evaporates as an Sb_2 molecule that has to dissociate at the surface in order to form a single layer, RT-deposition is suspected to leave some imperfections in the first layer, which most likely would escape detection in a LEED experiment. If such a local disorder were to be associated with band gap states, a very small density of the order of a thousands of a ML ($\approx 10^{12} \text{ cm}^{-2}$) of charged centers would be sufficient to create a Schottky-barrier at the interface.

For these reasons we performed high resolution core level studies on RT-deposited and annealed Sb/GaAs interfaces, which provide both a measure for the degree of perfection in the overlayer and precise information about the band bending at the interface. The former is achieved by a detailed lineshape analysis of the Sb-4d signal, while the band bending is derived from the energy shifts of the Ga-3d and As-3d bulk signals. The experiments were performed at the National Synchrotron Light Source (NSLS) in Brookhaven, New York; details of the experimental set-up have been published elsewhere⁽¹⁰⁾. Photoemission spectra were taken in an angle integrated mode under surface sensitive conditions (electron escape depths $\leq 5\text{\AA}$). The combined resolution of analyzer and monochromator was estimated to be $\leq 200\text{meV}$. Zn-doped (p-type) GaAs samples with a carrier concentration of $7 \cdot 10^{17} \text{ cm}^{-3}$ were cleaved *in situ* and tested for flatband condition. All samples used for further studies showed an initial deviation from flatband of $< 50\text{meV}$, resulting in a starting value of the Fermi-level

70:8 meV above VBM, as calculated from the bulk doping of the samples. Sb was evaporated from a BN effusion cell at typical rates of 0.3Å/min. Evaporation rates were calibrated by long term evaporation onto a quartz micro balance at the position of the sample. 1ML of Sb, defined as two atoms per GaAs surface unit cell ($\cong 8.85 \cdot 10^{14} \text{ cm}^{-2}$), corresponds to an equivalent thickness of 2.7Å. The Sb overlayers were grown at RT and could subsequently be annealed at temperatures up to 330°C. No changes were observed in the 1x1 LEED pattern upon annealing. The core level spectra were decomposed by means of a least-square fitting procedure ⁽¹⁾.

Fig.1 shows the changes in the Sb-4d spectra for various coverages before and after annealing at 330°C. Dots represent the data after subtraction of a smooth background, while the dashed and dash-dotted lines show the decomposition into two spin-orbit-split components; the solid lines give the sum of the components. Energy splitting and FWHM of the two Sb-4d components for an Sb coverage of 1Å ($\cong 0.4\text{ML}$) are plotted versus annealing temperature in Fig.2. Fig.3 shows energy splitting and FWHM as a function of coverage, which was obtained by sequential RT deposition and annealing at 330°C. This sequence leads not unexpectedly to slightly different values of the parameters at 1Å as compared to the data in Fig.2, which correspond to a single, uninterrupted deposition.

The development of the Sb-4d signal as a function of temperature and coverage reveals several interesting features: i) All spectra consist of two components. ii) The FWHM of both components narrows with increasing annealing temperature concomitant with an increase in their energy separation. An annealing temperature of 330°C is necessary to achieve maximum resolution of the components (see Fig.2). iii) The high kinetic energy (KE) component of the RT-deposited Sb overlayers becomes larger with respect to the low KE component for coverages

above $\approx 0.5\text{\AA}$ (see left panel in Fig.1) and finally remains the only surviving component for a thick Sb overlayer (not shown). After annealing at 330°C , the relation between the two components is reversed at lower coverages, but almost identical intensities are reached at 1ML (see right hand side of Fig.1).

The temperature and coverage dependent lineshape analysis of the Sb-4d core level allows direct conclusions about the changes in interface morphology induced by annealing. The splitting into two components, which was also observed by Myron *et al.* ⁽¹²⁾, results from the two different bonding sites in the first ML: According to the calculations ⁽⁴⁾ each Sb atom is covalently bonded to two Sb atoms along the zig-zag chain and has a third bond to either a Ga or an As atom of the topmost GaAs layer. The Sb-As bond is covalent, while the Sb-Ga bond has partly ionic character, with charge accumulation around the Sb atom. This results in a shift of all electronic states related to the Ga-site towards lower binding energies as compared to the states associated with the As-site ⁽⁴⁾. We therefore attribute the high KE component in the Sb-4d spectra (which corresponds to lower binding energy) to Sb atoms with a Ga bond, the other one to the As-sites. The perfect Sb ML is relaxed in a similar manner as the cleaved GaAs surface ⁽²⁾. For GaAs the relaxation results in a shift of the Ga-3d and As-3d binding energies of the topmost layer in opposite directions ⁽¹³⁾. We expect a similar behavior for the ordered Sb ML. Hence, the splitting in the two Sb-4d components should be largest for an ordered overlayer, while local nucleation on top of the first layer is expected to reduce the relaxation effect, resulting in a decrease of the splitting. Thus, we interpret the small splitting and the broadening of the components in the RT 4d-spectra as evidence for random nucleation on top of first layer Sb-atoms already at submonolayer coverages. Thermal annealing, on the other hand, enhances the surface mobility of the Sb atoms, resulting in a re-

duction of 3D-clusters and an increase of the ordered area. The highest annealing temperature studied (330°C) lies above the desorption threshold for Sb atoms above the first ML⁽³⁰⁾ and consequently suffices to remove all excess Sb. This argumentation is consistent with the changes observed in the intensity ratio of the components: Since the high KE component finally merges into the single signal found for a thick Sb overlayer, its larger intensity at low coverages for the unannealed samples appears consistent with a premature 3D growth. After annealing, the low KE component becomes larger, until equal intensity is reached at 1ML. This is a consequence of the higher surface mobility, which enables Sb atoms to reach energetically favorable binding sites. As the ordered Sb layer gets much of its binding energy from the Sb-Sb bonds along the chains⁽⁴⁾, the preference of the As-site is most likely limited to the end-positions of chains with random length distribution. The termination of the Sb chains at As-sites explains also the reduction in energy splitting and FWHM with coverage as is observed for the annealed films (Fig.3): The end-atoms in each chain lack one Sb-Sb bond and hence have smaller volume charge surrounding them. The associated change in binding energy results in a larger component splitting and apparent broadening at low coverage, where the percentage of end-atoms is largest. The absolute KE shifts of the two Sb-components support this interpretation: We find that the change in energy splitting results from the low KE component, while the other component follows the band bending within experimental error.

To study the influence of the overlayer morphology on the band bending at the interface, we measured the energy shift of the Ga-3d and As-3d core levels as a function of coverage for RT-deposited and annealed Sb overlayers. In either case, we find no evidence for chemical shifts in these levels. Both core levels consist only of a bulk and a surface component. The latter disappears, as expected, once

the surface is completely covered. Both bulk components show the same band bending shift within experimental uncertainty ($\leq \pm 40 \text{ meV}$). Fig.4a shows the Fermi-level shift with respect to VBM for unannealed Sb overlayers on a p-GaAs cleave. We observe a gradual increase in barrier height that reaches a value of 0.58 eV at 5 \AA coverage. Although the variation of barrier height with coverage is in good agreement with the results of RT-deposited films reported in Refs.6 and 8, we found relatively poor reproducibility with variations of up to 200 meV for different cleaves. Annealing affects the band bending significantly, as is shown in Fig.4b: In this experiment Sb was deposited at RT in several steps, followed by annealing after each deposition. PES spectra were recorded before and after annealing. We observe at all coverages a reduction in barrier height of up to a factor of two. The barrier of the annealed sample is almost independent of overlayer thickness in the accessible coverage range, resulting in a final pinning position of the Fermi-level 280 meV above VBM at 1ML. RT evaporation of more Sb on an annealed, 1ML thick Sb film almost re-establishes the barrier height that was observed before annealing. This process is reversible, i.e. subsequent annealing (concomitant with thermal desorption, which reduces the integrated intensity of the Sb-4d signal to the value at 1ML) results in the intrinsic barrier height of an ordered ML (see Fig.4).

The Sb-4d core level studies and the band bending experiments allow the following conclusions:

i) RT is not a suitable temperature to grow an ordered ML of Sb on GaAs(110). Films deposited at RT show local disorder and premature cluster growth on top of an incomplete first layer. This creates electronic states deep in the band gap, which pin the Fermi-level $\approx 0.6 \text{ eV}$ above VBM (p-GaAs).

ii) Annealing at temperatures above the desorption threshold for excess Sb leads to an ordered ML with a high degree of epitaxial perfection that reduces the pinning position to a value of 280meV above VBM. Valence band PES experiments with the proper band bending alignment show under these conditions Sb-derived emission in the band gap up to the Fermi-level⁽¹⁴⁾. This indicates that these states are responsible for the remaining barrier found on annealed samples. Hence we conclude that the highest filled Sb-states are located ≈ 300 meV higher than calculated in Refs. 4 and 5. With this intrinsic pinning position for an ordered Sb ML on p-GaAs, we can estimate the corresponding level for n-GaAs: Shifting the energetic position of the highest filled surface state found in the ARPES experiments⁽⁹⁾ into the gap by 300meV, in order to adjust it to our results, reduces their assumed value for the band bending on n-GaAs from 0.6eV to 0.3eV. This comparison is justified, because the ARPES experiments were also performed on annealed samples⁽⁹⁾.

iii) Although annealing reduces the Schottky-barrier on p-type and most likely also on n-type GaAs by about a factor of two, an ordered ML of Sb does not passivate the GaAs surface, but rather behaves like the topmost layer of the clean (110) surface itself: Deposition of more Sb, which resembles the partly 3D morphology of the unannealed films, shifts the Fermi-level several 100 meV higher into the band gap. We observe a similar behavior for Ag-deposition onto an annealed Sb film, which results in a pinning position close to the one observed for an Ag-covered GaAs(110) surface (see Fig.4).

The annealing experiments led to a consistent picture of the surface morphology of Sb overlayers on GaAs, which can explain most of the discrepancies in published results. However, the SPV measurements in Ref.7 are hard to reconcile with our conclusions: Although the reported reduction in barrier height seems

consistent with our results, we neither observe nor expect such a behavior upon RT-deposition, and certainly not for coverages beyond 1ML. It rather seems that SPV measurements, which actually measure workfunction changes of the overlayer, are not a proper technique to study the band bending on the GaAs-side of the interface. This conclusion is supported by the finding of semiconducting rather than metallic properties of up to 10ML thick Sb overlayers on GaAs^{(8),(15)}, which make an interpretation of SPV experiments ambiguous.

Acknowledgements

We thank M.Prikas and the staff of the NSLS for their technical assistance. This work was supported in part by the U.S. Army Research Office under contract No. DAAG-29-83-C-0026.

References

present addresses:

* Technische Universität München, Physik-Department E16, D-8046 Garching, FRG

* School for Physical Sciences, NIHE, Glasevin, Dublin 9, Ireland

* Universität München, Sektion Physik, D-8000 München, FRG

1. P.Skeath, C.Y.Su, I.Lindau, W.E.Spicer; *J. Vac. Sci. Technol.* 17, 874 (1980)
2. C.B.Duke, A.Paton, W.K.Ford; *Phys. Rev. B* 26, 803 (1982)
3. J.Carelli, A.Kahn; *Surf. Sci.* 116, 380 (1982)
4. C.M.Bertoni, C.Calandra, F.Manghi, E.Molinari; *Phys. Rev. B* 27, 1251 (1983)
5. C.Mailhot, C.B.Duke, D.J.Chadi; *Phys. Rev. Lett.* 53, 2114 (1984) *and Phys. Rev. B* 31, 2213 (1985)
6. M.Mattern-Klosson, H.Lüth; *Solid State Comm.* 56, 1001 (1985)
7. K.Li, A.Kahn; *J. Vac. Sci. Technol. A* 4, 958 (1986)
8. W.Pletschen, N.Esser, H.Münder, D.Zahn, J.Guerts, W.Richter; *Proc. of the 8th Europ. Conf. on Surf. Sci. (Surf. Sci. 1986)*
9. P.Mårtensson, G.V. Hansson, M.Lähdeniemi, K.O.Magnusson, S.Wiklund, J.M.Nicholls; *Phys. Rev. B* 33, 7399 (1986)
10. D.E.Eastman, J.J.Donelon, N.C.Hien, F.J.Himpsel; *Nuc. Instr. Methods* 172, 327 (1980); F.J.Himpsel, Y.Jugnet, D.E.Eastman, J.J.Donelon, D.Grimm, G.Landgren, A.Marx, J.F.Morar, C.Oden, R.A.Pollak, C.A.Schneir, C.A.Crider, *Nucl. Instr. Methods* 222, 107 (1984)
11. G.Landgren, R.Ludeke, Y.Jugnet, J.F.Morar, F.J.Himpsel; *J. Vac. Sci. Technol. B* 2, 351 (1984); R.Ludeke, G.Landgren; *Phys. Rev. B* 33, 5526 (1986)
12. J.R.Myron, J.Anderson, G.J.Lapeyre; *Proc. 17th Int. Conf. on the Phys. of Semicond. (Springer, New York 1985)*

13. D.E.Eastman, T.-C.Chiang, P.Heimann, F.J.Himpsel; Phys. Rev. Lett. 45, 656 (1980)
14. F.Schäffler, R.Ludeke, A.Taleb-Ibrahimi, D.Rieger; to be published
15. M.Mattem-Klosson, R.Stümpler, H.Lüth; Phys. Rev. B 33, 2559 (1986)

Figure Captions

- Fig.1* Comparison between Sb-4d spectra of RT-deposited Sb overlayers and spectra of the same films after annealing at 330°C. The dots represent the data, dashed and dash-dotted lines show the decomposition into the two components, which are summed up in the solid line. The highest coverage of 2.7Å corresponds to 1ML.
- Fig.2* Energy splitting and FWHM of the fitted Sb-4d components as a function of annealing temperature. The sample was covered with 1Å of Sb at RT and annealed at increasing temperatures.
- Fig.3* FWHM (a) and energy separation (b) of the two Sb-4d components for RT-deposited Sb overlayers before and after annealing at 330°C. The thickness of the annealed overlayers is desorption limited to 1ML (2.7Å).
- Fig.4* Fermi-level shift relative to VBM for Sb-covered p-GaAs cleaves. (a) Results for unannealed Sb overlayers on p-GaAs cleaves. (b) Influence of annealing: Sb was evaporated at RT resulting in the band bending represented by open symbols. Subsequent annealing lead to a significant reduction in barrier height (full symbols). Arrows indicate the sequence of the experiment.

Sb on p-GaAs(110)

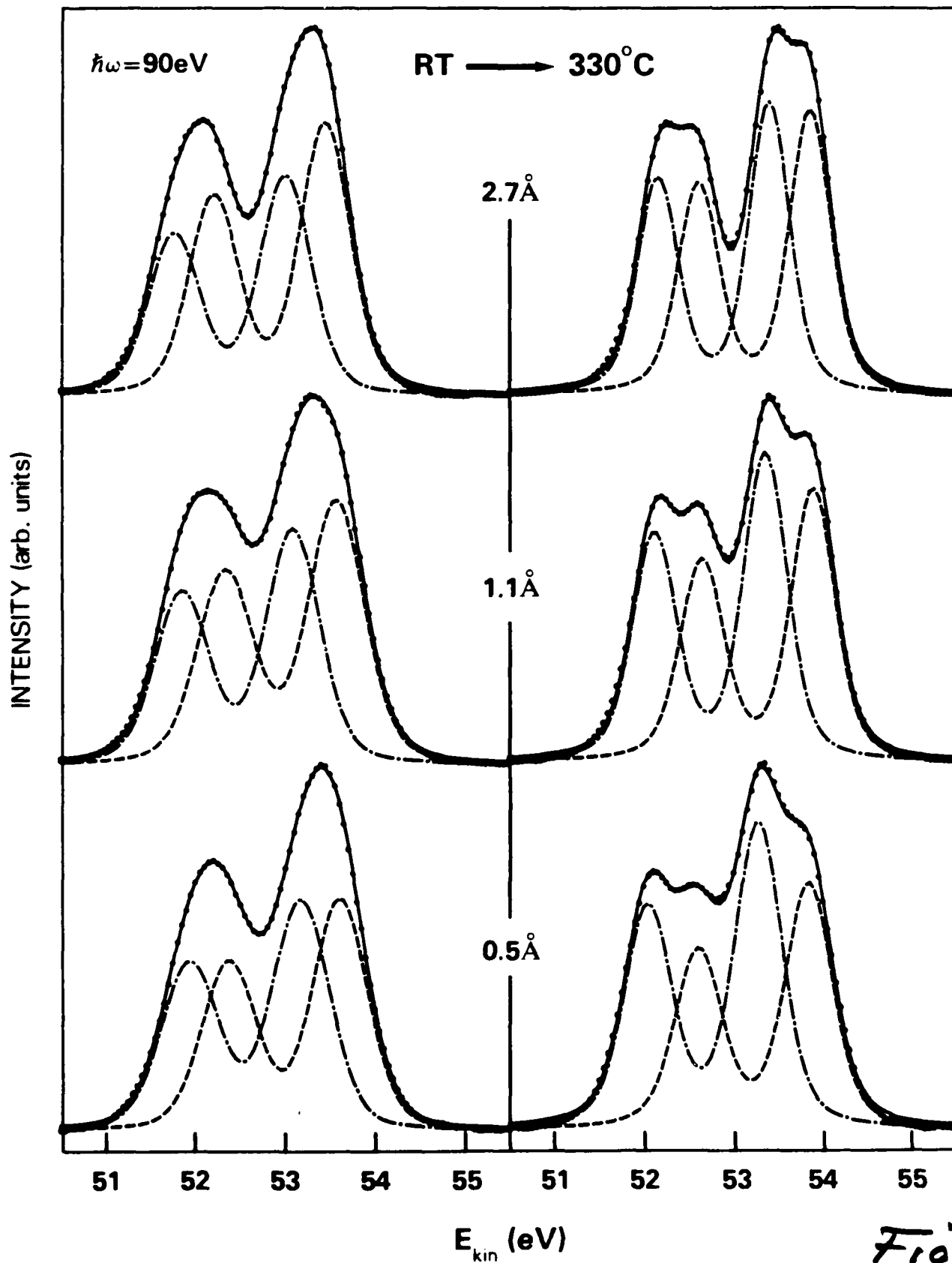


Fig. 1

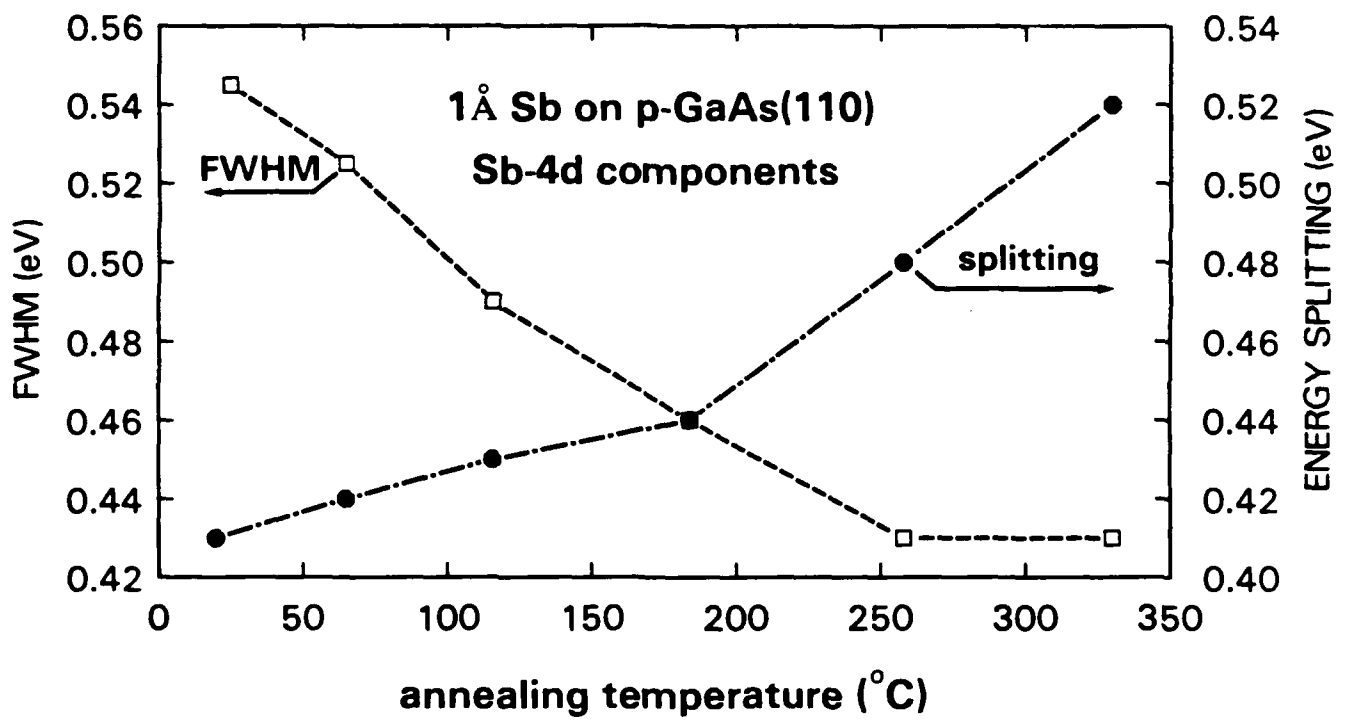


Fig. 2

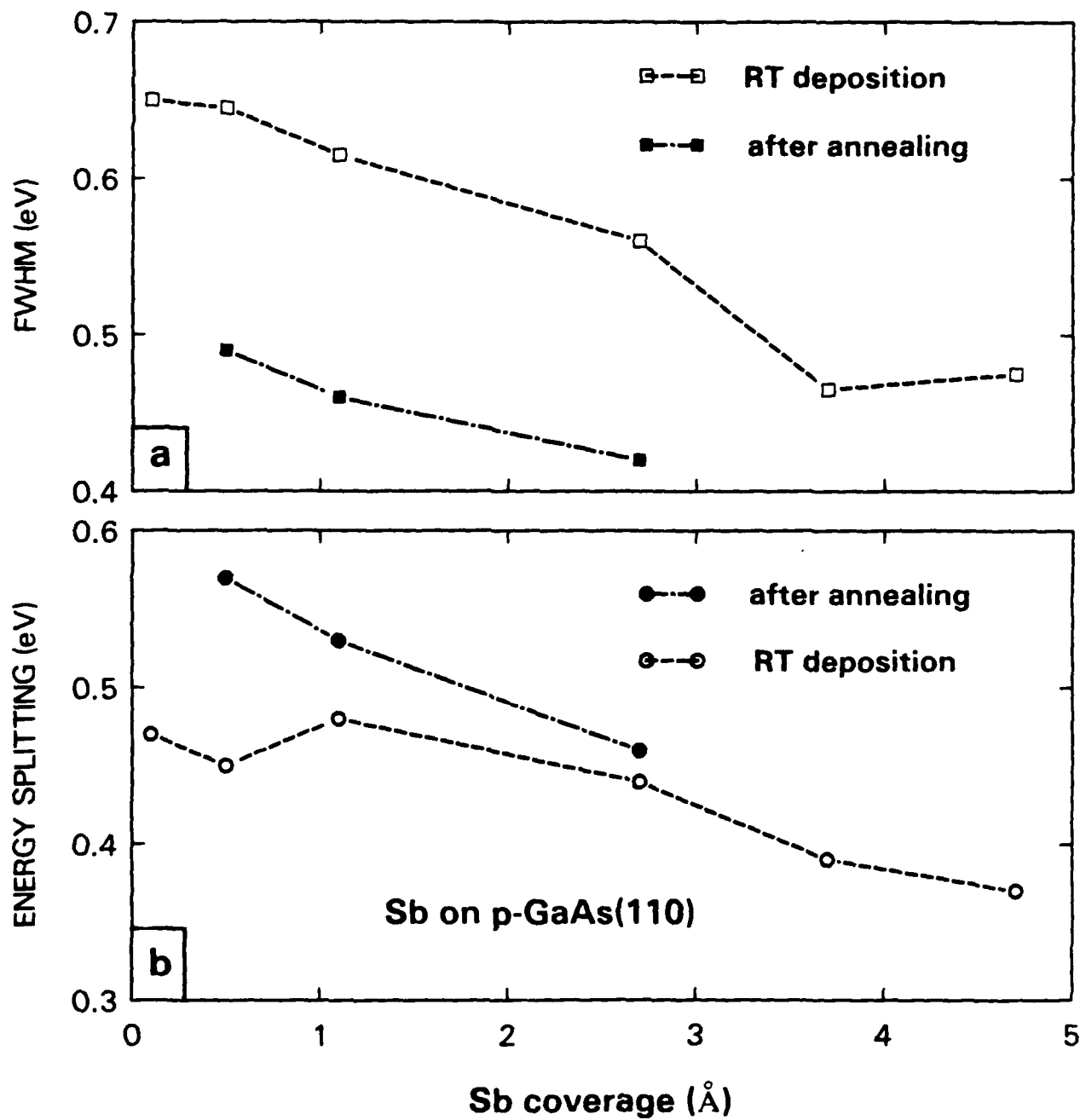


Fig. 3

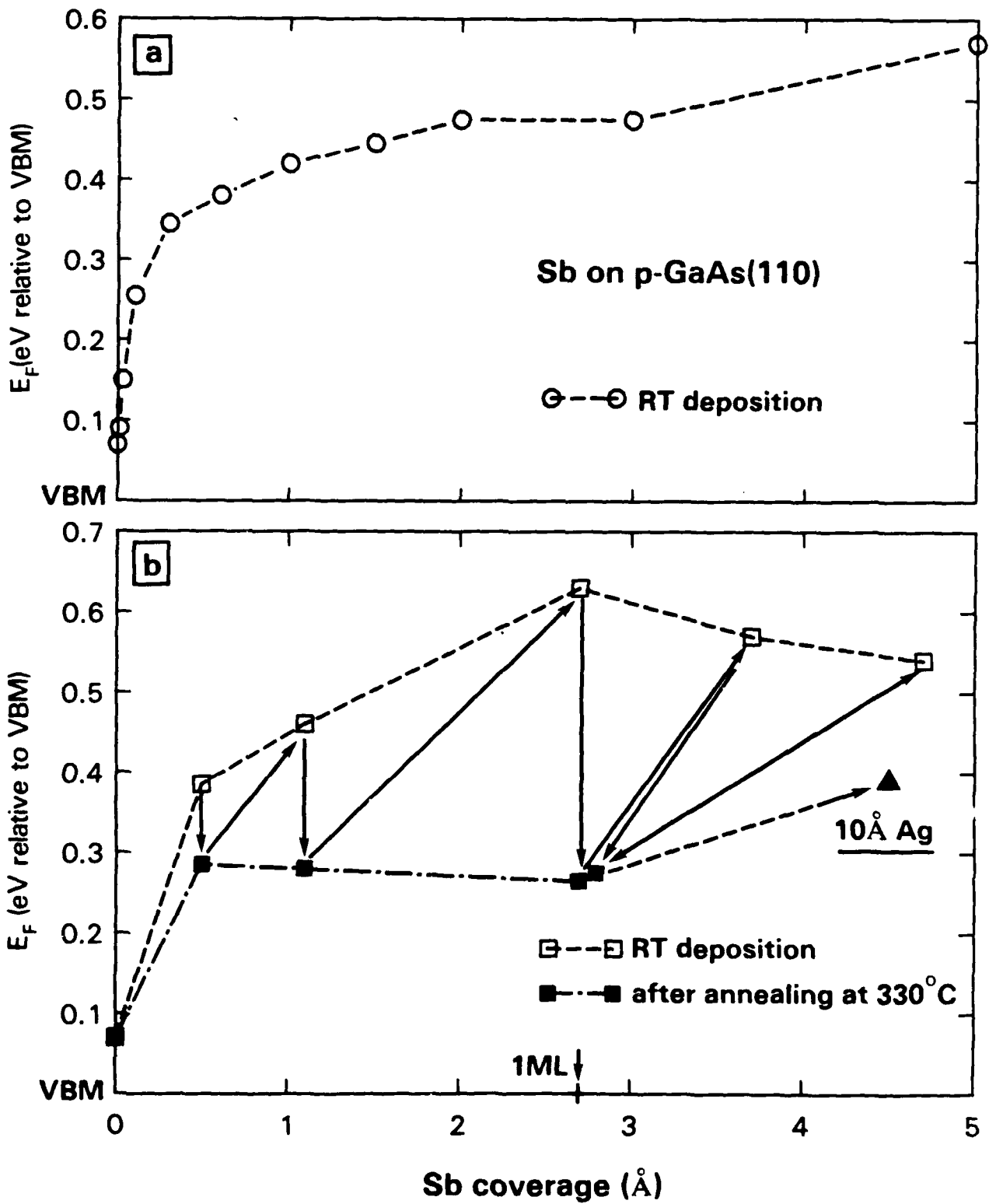


Fig. 4

END

3-87

DTIC